

# Graph-Enabled Fast MCMC Sampling with an Unknown High-Dimensional Prior Distribution

Chenyang Zhong\*

Department of Statistics, Columbia University  
cz2755@columbia.edu

and

Shouxuan Ji

Department of Statistics and Data Science, National University of Singapore  
shouxuan.ji@u.nus.edu

and

Tian Zheng\*

Department of Statistics, Columbia University  
tian.zheng@columbia.edu

August 6, 2024

## Abstract

Posterior sampling is a task of central importance in Bayesian inference. For many applications in Bayesian meta-analysis and Bayesian transfer learning, the prior distribution is unknown and needs to be estimated from samples. In practice, the prior distribution can be high-dimensional, adding to the difficulty of efficient posterior inference. In this paper, we propose a novel Markov chain Monte Carlo algorithm, which we term graph-enabled MCMC, for posterior sampling with unknown and potentially high-dimensional prior distributions. The algorithm is based on constructing a geometric graph from prior samples and subsequently uses the graph structure to guide the transition of the Markov chain. Through extensive theoretical and numerical studies, we demonstrate that our graph-enabled MCMC algorithm provides reliable approximation to the posterior distribution and is highly computationally efficient.

*Keywords:* Bayesian inference; high-dimensional unknown prior distribution; graph-based Markov chain Monte Carlo; kernel density estimation; Bayesian transfer learning

---

\*Corresponding authors

# 1 Introduction

The posterior distribution is a central object in Bayesian inference. Denoting by  $\theta \in \Theta \subseteq \mathbb{R}^d$  the parameter, and assuming that the prior distribution admits a density  $\pi(\theta)$ , the posterior density is given by

$$\pi(\theta|\mathbf{X}) = \frac{\pi(\theta)L(\theta|\mathbf{X})}{p(\mathbf{X})}, \quad \forall \theta \in \Theta,$$

where  $\mathbf{X} = (X_1, X_2, \dots, X_n)$  is the observed data,  $L(\theta|\mathbf{X})$  is the likelihood function, and

$$p(\mathbf{X}) = \int_{\Theta} \pi(\theta)L(\theta|\mathbf{X})d\theta \tag{1}$$

is the evidence. Oftentimes, the evidence  $p(\mathbf{X})$  cannot be evaluated in closed form, and it can be very costly to numerically compute the integral in (1). The situation is particularly challenging when the parameter space  $\Theta$  is high-dimensional, making exact posterior inference intractable. To resolve this difficulty, a commonly used method is to resort to obtaining approximate samples from the posterior distribution through Markov chain Monte Carlo (MCMC) algorithms and make inferences based on such samples (see e.g. Liu and Liu (2001); Brooks et al. (2011); Shahbaba et al. (2014)).

The above procedure applies to the ideal case where the prior density  $\pi(\theta)$  is known in exact form. In practice, however, there are many scenarios where the prior distribution is unknown and needs to be estimated from samples. For example, if we use the prior distribution to summarize historical data, oftentimes only posterior draws from Bayesian analysis of such data are available. As another example, when several research teams work on the same scientific problem, it is often beneficial to use posterior draws from previous studies to form a new prior for the current study; in such scenarios, concrete covariate and response data from previous studies are often unavailable, and even when such data are available, it would be computationally costly to directly use such data to retrain a

new posterior distribution. In Section 1.1, we present a motivating example on opioid use disorder data that belongs to the latter scenario. We also discuss the connections of the current problem to Bayesian meta-analysis and Bayesian transfer learning in Section 1.3.

In order to handle the unknown prior distribution, we consider the intuitive approach of using the kernel density estimate (KDE; see e.g. Rosenblatt (1956); Parzen (1962); Gramacki (2018)) based on prior samples to build an approximation to the posterior distribution. Denoting by  $\theta_1^{(0)}, \theta_2^{(0)}, \dots, \theta_B^{(0)} \in \mathbb{R}^d$  the  $B$  prior samples that are available to us, we propose to estimate the prior density  $\pi(\theta)$  by the kernel density estimate

$$\hat{\pi}_{\text{KDE}}(\theta) := \frac{1}{Bh^d} \sum_{i=1}^B K\left(\frac{\theta - \theta_i^{(0)}}{h}\right) \quad (2)$$

and build the following approximation to the true posterior  $\pi(\theta|\mathbf{X})$ :

$$\hat{\pi}(\theta|\mathbf{X}) \propto \left( \frac{1}{Bh^d} \sum_{i=1}^B K\left(\frac{\theta - \theta_i^{(0)}}{h}\right) \right) L(\theta|\mathbf{X}), \quad (3)$$

where  $K(\cdot)$  is a kernel on  $\mathbb{R}^d$  and  $h > 0$  is the kernel bandwidth (see Section 2.2 for details). We note that the flexibility offered by the nonparametric KDE is crucial for reliably estimating the posterior distribution, especially when the prior distribution is complex and multimodal. For instance, in Experiment I of Section 4, we consider posterior inference with an unknown Gaussian mixture prior distribution. Figure 1 compares the contour of the true posterior with the contours of approximate posteriors based on KDE (middle panel) and Gaussian estimate (estimating the prior by a Gaussian distribution; right panel) in this experiment; additional information on prior samples and the likelihood is presented in the left panel. As can be seen from this figure, the approximate posterior based on KDE closely matches the true posterior, while the one based on Gaussian estimate is significantly biased (in particular, note the shift of the posterior mode).

A direct approach based on the Metropolis-Hastings algorithm for sampling from the approximate posterior (3) is described in Section 1.2. One drawback of this approach is

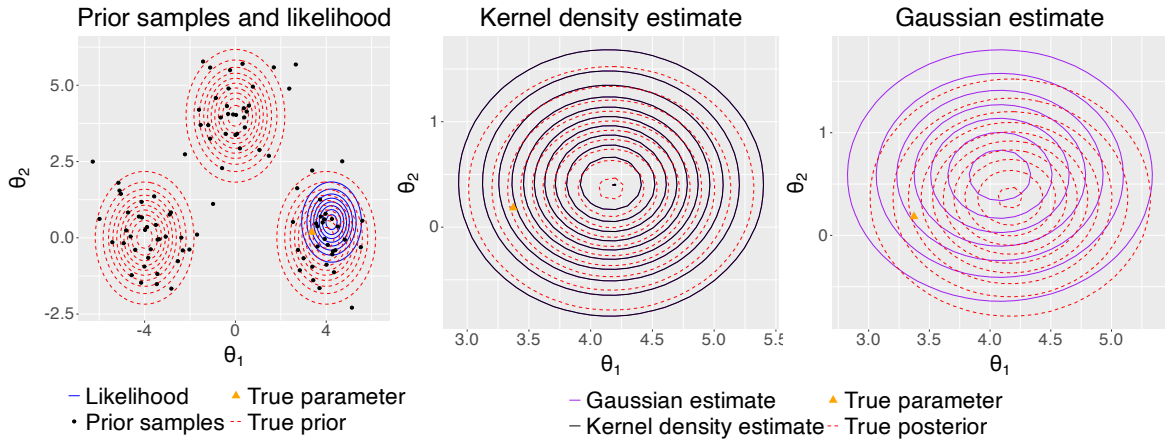


Figure 1: Prior samples and approximate posteriors

the computational cost, which scales up quickly in high-dimensional settings. To efficiently sample from (3), we introduce a novel MCMC algorithm that we term the “graph-enabled MCMC”. A salient feature of this algorithm is that it involves constructing a graph based on the locations of the prior samples and subsequently uses the graph structure to guide the transitions of the Markov chain. Through both theoretical analysis and numerical experiments, we demonstrate that the graph-enabled MCMC not only enables us to build a reliable approximation to the true posterior, but is also computationally much more efficient than alternative approaches.

## 1.1 Motivating example: estimating opioid use disorder epidemic using data from multiple sources

Opioid use disorder (OUD) has been prevalent in the United States for decades, raising ever-increasing concerns (Blanco and Volkow (2019); Strang et al. (2020)). Deaths by opioid overdose usually occur in individuals with OUD, making it crucial to estimate the prevalence of OUD for effective surveillance and treatment of opioid overdose. However, determining the prevalence of OUD, particularly the prevalence of “untreated” OUD, is

challenging when relying solely on public record data. Collecting alternative data is also difficult due to the stigma associated with OUD.

Recently, Doogan et al. (2022) carried out a study on the prevalence of OUD in the state of Ohio. Using linked health record data, they were able to derive a Bayesian model for estimating the prevalence of OUD among the Ohio population. Specifically, they proposed a regression model to estimate the overdose fatality risk for untreated OUD individuals in Ohio, and inferred the OUD prevalence using a multiplier method.

In this subsection, we briefly discuss an ongoing project in leveraging the fatal overdose data in the state of *New York* to infer the proportion of individuals with untreated OUD in this region. Different from Ohio, linked data are not available to carry out the same modeling strategy. Given the previous Ohio study in Doogan et al. (2022), it would be desirable to integrate the information from that study into our current study on OUD in New York. However, due to laws and regulations, data availability differs from state to state. Moreover, data cannot be easily shared between different states for the sake of data privacy and security. For these reasons, in the current study, we do not have access to the data used in the Ohio study but their model estimates.

Concretely, we adopt the following statistical model for fatal overdose in Ohio and New York. For each individual  $i$  with untreated OUD, we use  $y_i \in \{0, 1\}$  to indicate whether this individual dies ( $y_i = 1$ ) or not ( $y_i = 0$ ). The characteristics of this individual, such as the individual’s age, sex, and county of residence, is recorded as a  $d$ -dimensional feature vector  $\mathbf{x}_i = (x_{i1}, x_{i2}, \dots, x_{id})^\top$ . Given  $\mathbf{x}_i$ , the conditional distribution of  $y_i$  is assumed to be  $y_i | \mathbf{x}_i \stackrel{\text{ind}}{\sim} \text{Bernoulli} \left( \frac{e^{\mathbf{x}_i^\top \beta}}{1 + e^{\mathbf{x}_i^\top \beta}} \right)$ , where  $\beta \in \mathbb{R}^d$  is the model parameter. The Ohio study produces posterior draws of  $\beta \in \mathbb{R}^d$  using an uninformative prior and the data from Ohio. Taking the Ohio study as the *reference study*, the New York study (*current study*)

receives these posterior draws and uses them as prior information. The resulting posterior in New York would successfully incorporate the information from the reference study into the current study.

In later parts of this paper, we show that our proposed graph-enabled MCMC algorithm offers a highly computationally efficient approach to tackle this challenge. In particular, a numerical experiment motivated by the current example with  $d \in \{2, 6, 10\}$  is presented in Section 4, where we use the graph-enabled MCMC to estimate the New York posterior with informative prior as described above. In Figure 2, we compare this estimated posterior with the New York posterior with uninformative prior (i.e. without using the information in the Ohio study; see Section 4 for details). We also present the posterior samples from the Ohio study. We observe that the New York posterior with informative prior interpolates between the New York posterior with uninformative prior and the Ohio posterior samples, which shows that the New York posterior with informative prior successfully integrates the information from the Ohio study into the current New York study.

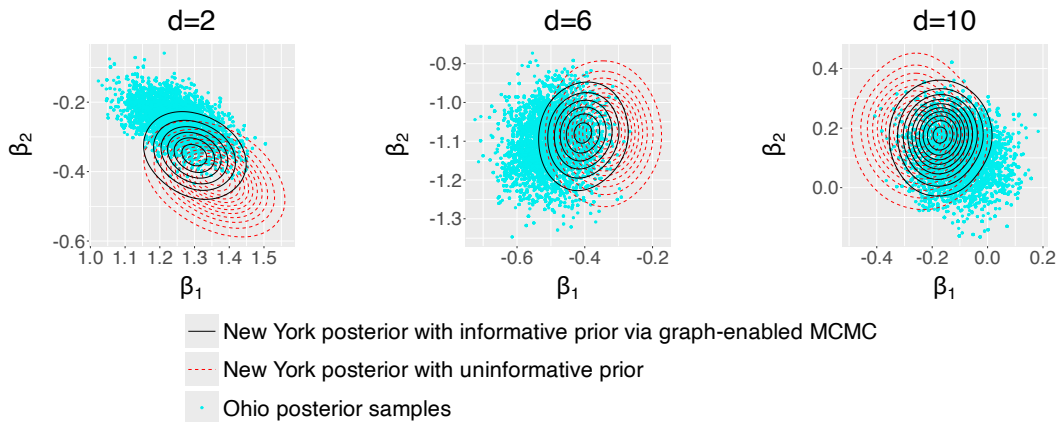


Figure 2: Ohio posterior samples and New York posteriors

## 1.2 Metropolis random walk with Gaussian proposal

A common approach for drawing samples from intractable posterior distributions is the Metropolis-Hastings algorithm (see e.g. Metropolis et al. (1953); Diaconis and Saloff-Coste (1995)). In our context of an unknown prior distribution, we may consider a Metropolis random walk with Gaussian proposal for sampling from the approximate posterior distribution  $\hat{\pi}(\theta|\mathbf{X})$  in (3). The algorithm depends on two tuning parameters  $\sigma_p, h > 0$ , and can be described as follows.

**Metropolis random walk with Gaussian proposal.** The random walk starts from  $\theta_0$  uniformly picked from  $\{\theta_1^{(0)}, \theta_2^{(0)}, \dots, \theta_B^{(0)}\}$ , and each step of the walk is given as follows. Suppose that the current state of the random walk is  $\theta_t$ . We sample  $\epsilon_t \sim \mathcal{N}(0, \sigma_p^2 I_d)$  (where  $I_d$  is the  $d \times d$  identity matrix), and take  $\theta'_t = \theta_t + \epsilon_t$ . Then we compute the kernel density estimate of  $\pi(\theta_t)$  and  $\pi(\theta'_t)$  by

$$\hat{\pi}_{\text{KDE}}(\theta_t) = \frac{1}{Bh^d} \sum_{i=1}^B K\left(\frac{\theta_t - \theta_i^{(0)}}{h}\right), \quad \hat{\pi}_{\text{KDE}}(\theta'_t) = \frac{1}{Bh^d} \sum_{i=1}^B K\left(\frac{\theta'_t - \theta_i^{(0)}}{h}\right).$$

The acceptance probability is  $\text{MH}_t = \min\left\{\frac{\hat{\pi}_{\text{KDE}}(\theta'_t)L(\theta'_t|\mathbf{X})}{\hat{\pi}_{\text{KDE}}(\theta_t)L(\theta_t|\mathbf{X})}, 1\right\}$ . With probability  $\text{MH}_t$ , the new state is  $\theta_{t+1} = \theta'_t$ ; with probability  $1 - \text{MH}_t$ , the new state is  $\theta_{t+1} = \theta_t$ . It can be verified that the stationary distribution of this Metropolis random walk is given by  $\hat{\pi}(\theta|\mathbf{X})$ .

Note that each iteration of the Metropolis random walk requires passing through all the  $B$  prior samples and performing  $2B$  kernel evaluations. In high dimensions, a large value of  $B$  is often needed to ensure accurate posterior approximation, and the computational cost of the current approach can be prohibitive. In Sections 3 and 4, we show that the graph-enabled MCMC is computationally much more efficient than the current approach.

### 1.3 Bayesian meta-analysis and Bayesian transfer learning

The case study presented in Section 1.1 forms an example of Bayesian meta-analysis. Broadly speaking, meta-analysis refers to a statistical analysis that combines the results of several studies (Borenstein et al. (2021); Zreik et al. (2010)). Bayesian methods, with the advantage of providing uncertainty quantification for parameters, is readily applicable to meta-analysis. In Bayesian meta-analysis, one can treat the posterior distribution from previous studies as a prior for the current study and combine this prior with the current data set to form a new posterior (see e.g. Wurpts et al. (2021); Schmid and Mengersen (2013); Kim et al. (2018)). As discussed above, in practice, it is usually the posterior draws rather than the exact posterior distribution that are available to us. Thus the graph-enabled MCMC algorithm provides an efficient tool for handling posterior inference in Bayesian meta-analysis.

The previous case study can also be put in the context of Bayesian transfer learning. In transfer learning, one has a source domain and a target domain, and the data distributions in these two domains differ (e.g. covariate shift or posterior shift). The goal is to leverage data in the source domain to enhance inference and prediction in the target domain. Recently, several methods have been introduced for performing transfer learning within the Bayesian framework (see e.g. Gönen and Margolin (2014); Karbalayghareh et al. (2018); Chandra and Kapoor (2020); Shwartz-Ziv et al. (2022)). Comprehensive surveys on Bayesian transfer learning can be found in Xuan et al. (2021); Suder et al. (2023). In our case study, we can view the reference study as the source domain and the current study as the target domain. We expect that our algorithm can be adapted to handle distributional shifts and perform transfer learning, and plan to explore these aspects in future works.

## 1.4 Organization of the paper

The rest of this paper is organized as follows. In Section 2, we formulate the problem setup and introduce the graph-enabled MCMC algorithm. Theoretical and computational properties of the algorithm, including validity of posterior approximation, explicit mixing time upper bounds, and computational complexity, are presented in Section 3. In Section 4, we evaluate the empirical performance of the algorithm through two numerical experiments. An application to a real data set on human behavior studies is presented in Section 5. Section 6 is devoted to the conclusions and the discussion of a practical extension for handling prior-likelihood distributional gaps.

## 2 Graph-enabled MCMC sampling

In this section, we introduce the graph-enabled MCMC algorithm. We introduce some notations and formulate the general problem setup in Section 2.1. Then in Section 2.2, we introduce two versions of the graph-enabled MCMC algorithm. The stationary distributions of the two MCMC algorithms are derived in Section 2.3. Finally, in Section 2.4, we describe an extension of the graph-enabled MCMC algorithm to the practical scenario where the parameters in the reference and current studies are only partially overlapping.

### 2.1 Notations and problem setup

Let  $\Theta \subseteq \mathbb{R}^d$  be the parameter space, where  $d$  is a positive integer, and let  $\mathcal{X}$  be the sample space. We assume a prior distribution on  $\Theta$  with density  $\pi(\cdot)$ , and the parameter  $\theta \in \Theta$  is drawn from this prior distribution. Given  $\theta$ , the observations  $X_1, X_2, \dots, X_n \in \mathcal{X}$  are generated i.i.d. from a distribution  $f(\cdot|\theta)$  (assumed to be known). Let  $\mathbf{X} := (X_1, X_2, \dots, X_n)$ .

Thus the likelihood function is  $L(\theta|\mathbf{X}) := \prod_{i=1}^n f(X_i|\theta)$  and the posterior distribution is  $\pi(\theta|\mathbf{X}) \propto \pi(\theta)L(\theta|\mathbf{X}) = \pi(\theta) \prod_{i=1}^n f(X_i|\theta)$ .

As discussed in the Introduction, there are many practical scenarios where the exact form of the prior density  $\pi(\cdot)$  is not available to us. Instead, what we have about the prior is a series of i.i.d. samples  $\theta_1^{(0)}, \theta_2^{(0)}, \dots, \theta_B^{(0)}$  drawn from  $\pi(\cdot)$ . Hereafter, we denote  $\Theta_0 := \{\theta_1^{(0)}, \theta_2^{(0)}, \dots, \theta_B^{(0)}\}$ . Our goal is to develop an algorithm for approximately sampling from the posterior  $\pi(\cdot|\mathbf{X})$  based on  $\Theta_0$  and  $\mathbf{X}$ .

## 2.2 Graph-enabled MCMC algorithm

In this subsection, we describe the graph-enabled MCMC algorithm for approximately sampling from the posterior distribution  $\pi(\cdot|\mathbf{X})$  based on  $\Theta_0$  and  $\mathbf{X}$ . The algorithm depends on the following parameters: the number of prior samples,  $B$ ; the number of nearest neighbors used to construct the graph,  $k \in \mathbb{N}^*$ ; the probability of proposing to restart the random walk on the graph from a uniformly chosen vertex,  $\rho \in (0, 1)$ ; a kernel on  $\mathbb{R}^d$ ,  $K(\cdot)$ , satisfying  $\int_{\mathbb{R}^d} K(u)du = 1$  and  $K(u) \geq 0, \forall u \in \mathbb{R}^d$ ; the kernel bandwidth,  $h > 0$ ; and the number of posterior draws that we wish to obtain,  $N$ . An example of  $K(u)$  is the Gaussian density:

$$K(u) = (2\pi)^{-d/2} \exp(-\|u\|^2/2), \quad \forall u \in \mathbb{R}^d. \quad (4)$$

The first step of the algorithm involves constructing an undirected graph  $G_k$  with vertex set  $\Theta_0$  and edge set  $E_k$ . We describe the construction as follows. Hereafter, we denote  $[m] := \{1, \dots, m\}$  for any positive integer  $m$ . For any  $i \in [B]$ , we denote by  $\mathcal{N}_k(\theta_i^{(0)})$  the set of  $k$  nodes in  $\Theta_0 \setminus \{\theta_i^{(0)}\}$  that are closest in Euclidean distance to  $\theta_i^{(0)}$ . For any two distinct nodes  $\theta_i^{(0)}, \theta_j^{(0)} \in \Theta_0$  (where  $i, j \in [B]$ ), we connect them with an edge (i.e.  $\{\theta_i^{(0)}, \theta_j^{(0)}\} \in E_k$ ) if  $\theta_i^{(0)} \in \mathcal{N}_k(\theta_j^{(0)})$  or  $\theta_j^{(0)} \in \mathcal{N}_k(\theta_i^{(0)})$ . For any  $i \in [B]$ , we denote by  $D_k(\theta_i^{(0)})$

the degree of the node  $\theta_i^{(0)}$  in the graph  $G_k$ .

For the remaining procedures, we propose two alternatives, resulting in two versions of the algorithm. The first version, which we term “graph-enabled discretized MCMC”, is a kernel smoothed version of a random walk on the graph  $G_k$  and is simpler to implement. The second version, termed “graph-enabled MCMC”, is a graph-assisted random walk in the continuous space. As the actual posterior resides in a continuous space, this version provides a more accurate approximation to the true posterior (see Section 2.3 for details).

In the following, we describe the two alternatives separately. For any  $\theta^{(0)} \in \Theta_0$ , we let  $p_{\theta^{(0)},h}(\cdot)$  be the distribution on  $\mathbb{R}^d$  given by

$$p_{\theta^{(0)},h}(\theta) = \frac{1}{h^d} K\left(\frac{\theta - \theta^{(0)}}{h}\right), \quad \forall \theta \in \mathbb{R}^d. \quad (5)$$

**Algorithm I: graph-enabled discretized MCMC** We pick a node  $\theta_{(0)}^{(0)}$  uniformly at random from  $\Theta_0$ . Sequentially for each  $t \in [N]$ , assuming that  $\theta_{(t-1)}^{(0)}$  has been determined, we do the following:

1. With probability  $\rho$ , we draw  $\alpha_t$  uniformly from  $\Theta_0$ ; with probability  $1 - \rho$ , we draw  $\alpha_t$  uniformly from the neighbors of  $\theta_{(t-1)}^{(0)}$  in the graph  $G_k$ .

2. Compute the acceptance probability

$$\text{MH}_t = \min \left\{ \frac{\frac{\rho}{B} + \frac{1-\rho}{D_k(\alpha_t)} \mathbb{1}_{\{\theta_{(t-1)}^{(0)}, \alpha_t\} \in E_k}}}{\frac{\rho}{B} + \frac{1-\rho}{D_k(\theta_{(t-1)}^{(0)})} \mathbb{1}_{\{\theta_{(t-1)}^{(0)}, \alpha_t\} \in E_k}} \cdot \frac{L(\alpha_t | \mathbf{X})}{L(\theta_{(t-1)}^{(0)} | \mathbf{X})}, 1 \right\}.$$

With probability  $\text{MH}_t$ , we let  $\theta_{(t)}^{(0)} = \alpha_t$ ; with probability  $1 - \text{MH}_t$ , we let  $\theta_{(t)}^{(0)} = \theta_{(t-1)}^{(0)}$ .

Thus we obtain  $\{\theta_{(t)}^{(0)}\}_{t=1}^N$ . For each  $t \in [N]$ , we draw  $\theta_t^{(1)}$  from the distribution  $p_{\theta_{(t)}^{(0)},h}(\cdot)$  (see (5)). Our desired samples are  $\{\theta_t^{(1)}\}_{t=1}^N$ .

**Algorithm II: graph-enabled MCMC** We define a Markov chain on  $\Theta_0 \times \mathbb{R}^d$ . We pick a node  $\theta_{(0)}^{(0)}$  uniformly at random from  $\Theta_0$  and draw  $\theta_0^{(1)}$  from the distribution  $p_{\theta_{(0)}^{(0)},h}(\cdot)$ . Sequentially for each  $t \in [N]$ , assuming that  $\theta_{(t-1)}^{(0)}$  and  $\theta_{t-1}^{(1)}$  have been determined, we do the following:

1. With probability  $\rho$ , we draw  $\alpha_t$  uniformly from  $\Theta_0$ ; with probability  $1 - \rho$ , we draw  $\alpha_t$  uniformly from the neighbors of  $\theta_{(t-1)}^{(0)}$  in the graph  $G_k$ .
2. We draw  $\tilde{\alpha}_t$  from the distribution  $p_{\alpha_t,h}(\cdot)$ .
3. Compute the acceptance probability

$$\text{MH}_t = \min \left\{ \frac{\frac{\rho}{B} + \frac{1-\rho}{D_k(\alpha_t)} \mathbb{1}_{\{\theta_{(t-1)}^{(0)}, \alpha_t\} \in E_k}}}{\frac{\rho}{B} + \frac{1-\rho}{D_k(\theta_{(t-1)}^{(0)})} \mathbb{1}_{\{\theta_{(t-1)}^{(0)}, \alpha_t\} \in E_k}} \cdot \frac{L(\tilde{\alpha}_t|\mathbf{X})}{L(\theta_{t-1}^{(1)}|\mathbf{X})}, 1 \right\}. \quad (6)$$

With probability  $\text{MH}_t$ , we let  $\theta_{(t)}^{(0)} = \alpha_t$  and  $\theta_t^{(1)} = \tilde{\alpha}_t$ ; with probability  $1 - \text{MH}_t$ , we let  $\theta_{(t)}^{(0)} = \theta_{(t-1)}^{(0)}$  and  $\theta_t^{(1)} = \theta_{t-1}^{(1)}$ .

Our desired samples are  $\{\theta_t^{(1)}\}_{t=1}^N$ . The entire algorithm is summarized in Algorithm 1.

---

**Algorithm 1** Graph-enabled MCMC

---

- 1: To initialize, construct the graph  $G_k$ .
  - 2:  $t \leftarrow 0$ , draw  $\theta_{(t)}^{(0)}$  uniformly from  $\Theta_0$  and  $\theta_t^{(1)}$  from the distribution  $p_{\theta_{(t)}^{(0)},h}(\cdot)$ .
  - 3: **for**  $t = 1, 2, \dots, N$  **do**
  - 4:     With probability  $\rho$ , draw  $\alpha_t$  uniformly from  $\Theta_0$ ; otherwise draw  $\alpha_t$  uniformly from the neighbors of  $\theta_{(t-1)}^{(0)}$  in  $G_k$ . Then draw  $\tilde{\alpha}_t$  from the distribution  $p_{\alpha_t,h}(\cdot)$ .
  - 5:     Compute  $\text{MH}_t$  using (6), and accept the move from  $(\theta_{(t-1)}^{(0)}, \theta_{t-1}^{(1)})$  to  $(\alpha_t, \tilde{\alpha}_t)$  with probability  $\text{MH}_t$ .
  - 6: **end for**
-

## 2.3 Stationary distribution of the graph-enabled MCMC

In this subsection, we describe the stationary distributions of the two versions of the graph-enabled MCMC algorithm. We have the following two propositions.

**Proposition 2.1.** *The stationary distribution of  $\theta_t^{(1)}$  in the graph-enabled discretized MCMC (Algorithm I) is*

$$\tilde{\pi}(\theta|\mathbf{X}) \propto \frac{1}{Bh^d} \sum_{i=1}^B K\left(\frac{\theta - \theta_i^{(0)}}{h}\right) L(\theta_i^{(0)}|\mathbf{X}), \quad \forall \theta \in \mathbb{R}^d. \quad (7)$$

*Proof.* Based on the theory of the Metropolis-Hastings algorithm, the stationary distribution of  $\theta_{(t)}^{(0)}$  on  $\Theta_0$  is proportional to  $L(\theta_{(t)}^{(0)}|\mathbf{X})$ . As  $\theta_t^{(1)}$  is drawn from  $p_{\theta_{(t)}^{(0)},h}(\cdot)$ , the stationary distribution of  $\theta_t^{(1)}$  is given by (7). □

**Proposition 2.2.** *The stationary distribution of  $\theta_t^{(1)}$  in the graph-enabled MCMC (Algorithm II) is*

$$\hat{\pi}(\theta|\mathbf{X}) \propto \left( \frac{1}{Bh^d} \sum_{i=1}^B K\left(\frac{\theta - \theta_i^{(0)}}{h}\right) \right) L(\theta|\mathbf{X}), \quad \forall \theta \in \mathbb{R}^d. \quad (8)$$

*Proof.* Based on the theory of the Metropolis-Hastings algorithm, the stationary distribution of  $(\theta_{(t)}^{(0)}, \theta_t^{(1)})$  on  $\Theta_0 \times \mathbb{R}^d$  is proportional to  $h^{-d} K((\theta_t^{(1)} - \theta_{(t)}^{(0)})/h) L(\theta_t^{(1)}|\mathbf{X})$ . We obtain the conclusion by marginalizing out  $\theta_{(t)}^{(0)} \in \Theta_0$ . □

From the two propositions above, we note that the second and more complicated version of the algorithm provides a more accurate approximation to the true posterior. Theoretical guarantees on the validity of the algorithm for posterior approximation will be presented in Section 3.1.

## 2.4 Extension to partially overlapping parameters across different studies

Quite often in practice, different research teams can develop different kinds of models to address the same scientific problem. This can lead to distinct sets of parameters across such studies. In this subsection, we describe an extension of our graph-enabled MCMC algorithm for such scenarios.

For notational simplicity, we consider the case of two studies. We denote by  $(\theta_S, \theta_C)$  the set of parameters for the reference study and  $(\theta_T, \theta_C)$  the set of parameters for the current study, where  $\theta_C \in \mathbb{R}^d$  consists of parameters that are shared across the two studies and  $\theta_S \in \mathbb{R}^{d_1}, \theta_T \in \mathbb{R}^{d_2}$  are parameters unique to each study. As in Section 2.1, we denote the observations by  $\mathbf{X} = (X_1, X_2, \dots, X_n)$  and the posterior draws from the reference study by  $\Theta_0 = \{\theta_1^{(0)}, \theta_2^{(0)}, \dots, \theta_B^{(0)}\}$ . We also assume a prior distribution  $\pi_T(\cdot)$  for  $\theta_T$ .

We adapt the graph-enabled MCMC algorithm to the current setup as follows. In addition to the parameters introduced in Section 2.2, the algorithm depends on an extra parameter  $\sigma > 0$ . For each  $i \in [B]$ , we write  $\theta_i^{(0)} = (\theta_{i,S}^{(0)}, \theta_{i,C}^{(0)})$ . We keep the shared parameters  $\Theta_{0,C} := \{\theta_{1,C}^{(0)}, \dots, \theta_{B,C}^{(0)}\}$ . Then we construct a graph  $G_k$  with vertex set  $\Theta_{0,C}$  following a similar procedure as in Section 2.2. We pick  $\theta_{(0),C}^{(0)}$  uniformly from  $\Theta_{0,C}$  and draw  $\theta_{0,C}^{(1)}$  from the distribution  $p_{\theta_{(0),C}^{(0)}, h}(\cdot)$  (see (5)). We also select an arbitrary initial value  $\theta_{0,T}^{(1)} \in \mathbb{R}^{d_2}$ . Sequentially for each  $t \in [N]$ , assuming that  $\theta_{(t-1),C}^{(0)}, \theta_{t-1,C}^{(1)}, \theta_{t-1,T}^{(1)}$  have been determined, we do the following:

1. With probability  $\rho$ , we draw  $\alpha_{t,C}$  uniformly from  $\Theta_{0,C}$ ; with probability  $1 - \rho$ , we draw  $\alpha_{t,C}$  uniformly from the neighbors of  $\theta_{(t-1),C}^{(0)}$  in the graph  $G_k$ . Then we draw  $\tilde{\alpha}_{t,C}$  from the distribution  $p_{\alpha_{t,C}, h}(\cdot)$ .

2. We sample  $\epsilon_t \sim \mathcal{N}(0, \sigma^2 I_{d_2})$ , and take  $\tilde{\alpha}_{t,T} = \theta_{t-1,T}^{(1)} + \epsilon_t$ .

3. Compute the acceptance probability

$$\text{MH}_t = \min \left\{ \frac{\frac{\rho}{B} + \frac{1-\rho}{D_k(\alpha_{t,C})} \mathbb{1}_{\{\theta_{(t-1),C}^{(0)}, \alpha_{t,C}\} \in E_k}}}{\frac{\rho}{B} + \frac{1-\rho}{D_k(\theta_{(t-1),C}^{(0)})} \mathbb{1}_{\{\theta_{(t-1),C}^{(0)}, \alpha_{t,C}\} \in E_k}} \cdot \frac{L((\tilde{\alpha}_{t,T}, \tilde{\alpha}_{t,C})|\mathbf{X})}{L((\theta_{t-1,T}^{(1)}, \theta_{t-1,C}^{(1)})|\mathbf{X})} \cdot \frac{\pi_T(\tilde{\alpha}_{t,T})}{\pi_T(\theta_{t-1,T}^{(1)})}, 1 \right\}.$$

With probability  $\text{MH}_t$ , we let  $\theta_{(t),C}^{(0)} = \alpha_{t,C}$ ,  $\theta_{t,C}^{(1)} = \tilde{\alpha}_{t,C}$ , and  $\theta_{t,T}^{(1)} = \tilde{\alpha}_{t,T}$ ; with probability  $1 - \text{MH}_t$ , we let  $\theta_{(t),C}^{(0)} = \theta_{(t-1),C}^{(0)}$ ,  $\theta_{t,C}^{(1)} = \theta_{t-1,C}^{(1)}$ , and  $\theta_{t,T}^{(1)} = \theta_{t-1,T}^{(1)}$ .

Let  $\theta_t^{(1)} := (\theta_{t,T}^{(1)}, \theta_{t,C}^{(1)})$  for each  $t \in [N]$ . Our desired samples are  $\{\theta_t^{(1)}\}_{t=1}^N$ .

We have the following proposition on the stationary distribution of the generalized algorithm. The proof of this proposition is similar to that of Proposition 2.2.

**Proposition 2.3.** *The stationary distribution of  $\theta_t^{(1)}$  in the preceding algorithm is*

$$\hat{\pi}(\theta|\mathbf{X}) \propto \pi_T(\theta_T) \left( \frac{1}{Bh^d} \sum_{i=1}^B K \left( \frac{\theta_C - \theta_{i,C}^{(0)}}{h} \right) \right) L(\theta|\mathbf{X}), \quad \forall \theta = (\theta_T, \theta_C) \in \mathbb{R}^{d+d_2}.$$

### 3 Theoretical and computational properties

In this section, we establish theoretical and computational properties of the graph-enabled MCMC algorithm introduced in Section 2.2. In Section 3.1, we show that the stationary distributions of both versions of the algorithm closely approximate the true posterior distribution under mild conditions. Then we provide explicit mixing time upper bounds for both versions of the algorithm in Section 3.2, which demonstrate that the algorithm is rapidly mixing in practical scenarios. Finally, in Section 3.3, we analyze the computational complexity of the algorithm and compare it with that of the Metropolis random walk.

Throughout this section, we assume a given set of observations  $\mathbf{X}$ , and relevant expectations and probabilities are with respect to the randomness in  $\{\theta_i^{(0)}\}_{i=1}^B$ . We also assume that the parameter space  $\Theta = \mathbb{R}^d$  and  $\int_{\mathbb{R}^d} \pi(\theta) L(\theta|\mathbf{X}) d\theta \in (0, \infty)$  (note that the latter is necessary for the posterior density to exist).

### 3.1 Validity of posterior approximation

In this subsection, we show that the stationary distributions of both versions of the graph-enabled MCMC algorithm ( $\tilde{\pi}(\theta|\mathbf{X})$  and  $\hat{\pi}(\theta|\mathbf{X})$ ; see Section 2.3) provide close approximations to the true posterior  $\pi(\theta|\mathbf{X})$  under mild conditions. The following theorem establishes the consistency of  $\hat{\pi}(\theta|\mathbf{X})$  in estimating  $\pi(\theta|\mathbf{X})$  in the asymptotic regime where  $B \rightarrow \infty$ ,  $h \rightarrow 0$ , and  $Bh^d \rightarrow \infty$ .

**Theorem 3.1.** *Assume that  $\sup_{\theta \in \mathbb{R}^d} L(\theta|\mathbf{X}) < \infty$ . Additionally, assume that  $h \rightarrow 0$  and  $Bh^d \rightarrow \infty$  as  $B \rightarrow \infty$ . Then we have  $\lim_{B \rightarrow \infty} \mathbb{E} \left[ \int_{\mathbb{R}^d} |\hat{\pi}(\theta|\mathbf{X}) - \pi(\theta|\mathbf{X})| d\theta \right] = 0$ .*

*Proof.* Recall the definition of  $\hat{\pi}_{\text{KDE}}(\theta)$  from (2). We note that for any  $\theta \in \mathbb{R}^d$ ,

$$\begin{aligned} |\hat{\pi}(\theta|\mathbf{X}) - \pi(\theta|\mathbf{X})| &= \left| \frac{\hat{\pi}_{\text{KDE}}(\theta)L(\theta|\mathbf{X})}{\int_{\mathbb{R}^d} \hat{\pi}_{\text{KDE}}(\tau)L(\tau|\mathbf{X})d\tau} - \frac{\pi(\theta)L(\theta|\mathbf{X})}{\int_{\mathbb{R}^d} \pi(\tau)L(\tau|\mathbf{X})d\tau} \right| \\ &\leq \left| \frac{\hat{\pi}_{\text{KDE}}(\theta)L(\theta|\mathbf{X})}{\int_{\mathbb{R}^d} \hat{\pi}_{\text{KDE}}(\tau)L(\tau|\mathbf{X})d\tau} - \frac{\hat{\pi}_{\text{KDE}}(\theta)L(\theta|\mathbf{X})}{\int_{\mathbb{R}^d} \pi(\tau)L(\tau|\mathbf{X})d\tau} \right| + \left| \frac{\hat{\pi}_{\text{KDE}}(\theta)L(\theta|\mathbf{X})}{\int_{\mathbb{R}^d} \pi(\tau)L(\tau|\mathbf{X})d\tau} - \frac{\pi(\theta)L(\theta|\mathbf{X})}{\int_{\mathbb{R}^d} \pi(\tau)L(\tau|\mathbf{X})d\tau} \right| \\ &\leq \frac{\hat{\pi}_{\text{KDE}}(\theta)L(\theta|\mathbf{X}) \int_{\mathbb{R}^d} |\hat{\pi}_{\text{KDE}}(\tau) - \pi(\tau)|L(\tau|\mathbf{X})d\tau}{\int_{\mathbb{R}^d} \hat{\pi}_{\text{KDE}}(\tau)L(\tau|\mathbf{X})d\tau \int_{\mathbb{R}^d} \pi(\tau)L(\tau|\mathbf{X})d\tau} + \frac{|\hat{\pi}_{\text{KDE}}(\theta) - \pi(\theta)|L(\theta|\mathbf{X})}{\int_{\mathbb{R}^d} \pi(\tau)L(\tau|\mathbf{X})d\tau}. \end{aligned}$$

Hence

$$\begin{aligned} \int_{\mathbb{R}^d} |\hat{\pi}(\theta|\mathbf{X}) - \pi(\theta|\mathbf{X})| d\theta &\leq \frac{2 \int_{\mathbb{R}^d} |\hat{\pi}_{\text{KDE}}(\theta) - \pi(\theta)|L(\theta|\mathbf{X})d\theta}{\int_{\mathbb{R}^d} \pi(\theta)L(\theta|\mathbf{X})d\theta} \\ &\leq \frac{2 \sup_{\theta \in \mathbb{R}^d} L(\theta|\mathbf{X})}{\int_{\mathbb{R}^d} \pi(\theta)L(\theta|\mathbf{X})d\theta} \int_{\mathbb{R}^d} |\hat{\pi}_{\text{KDE}}(\theta) - \pi(\theta)| d\theta. \quad (9) \end{aligned}$$

By (Devroye and Lugosi, 2001, Theorem 9.2),  $\lim_{B \rightarrow \infty} \mathbb{E} \left[ \int_{\mathbb{R}^d} |\hat{\pi}_{\text{KDE}}(\theta) - \pi(\theta)| d\theta \right] = 0$ .

Noting (9), we conclude that as  $B \rightarrow \infty$ ,

$$\mathbb{E} \left[ \int_{\mathbb{R}^d} |\hat{\pi}(\theta|\mathbf{X}) - \pi(\theta|\mathbf{X})| d\theta \right] \leq \frac{2 \sup_{\theta \in \mathbb{R}^d} L(\theta|\mathbf{X})}{\int_{\mathbb{R}^d} \pi(\theta)L(\theta|\mathbf{X})d\theta} \mathbb{E} \left[ \int_{\mathbb{R}^d} |\hat{\pi}_{\text{KDE}}(\theta) - \pi(\theta)| d\theta \right] \rightarrow 0.$$

□

The following theorem shows that  $\tilde{\pi}(\theta|\mathbf{X})$  is close to  $\hat{\pi}(\theta|\mathbf{X})$  under additional regularity assumptions. We defer the proof to Section A.1 of the supplementary material.

**Theorem 3.2.** *Assume that  $\sup_{\theta \in \mathbb{R}^d} L(\theta|\mathbf{X}) < \infty$ ,  $\int_{\mathbb{R}^d} K(u)\|u\|_2 du < \infty$ , and  $L(\theta|\mathbf{X})$  is  $M$ -Lipschitz as a function of  $\theta \in \mathbb{R}^d$  (where  $M$  is a fixed positive constant). Additionally, assume that  $B \rightarrow \infty$  and  $h \rightarrow 0$ . Then  $\int_{\mathbb{R}^d} |\tilde{\pi}(\theta|\mathbf{X}) - \hat{\pi}(\theta|\mathbf{X})| d\theta \xrightarrow{P} 0$ .*

## 3.2 Mixing time analysis

For MCMC algorithms, determining the number of iterations required for the Markov chain to approach stationarity is crucial. This initial period, known as the “burn-in” phase, is typically characterized by the total variation mixing time (Levin and Peres (2017)). For the graph-enabled discretized MCMC (Algorithm I), we denote by  $P_d^t$  the distribution of  $\theta_{(t)}^{(0)}$  for each  $t \in \mathbb{N}$ , and denote by  $\pi_d$  the stationary distribution of  $\theta_{(t)}^{(0)}$ . For the graph-enabled MCMC (Algorithm II), we denote by  $P_c^t$  the distribution of  $(\theta_{(t)}^{(0)}, \theta_t^{(1)})$  for each  $t \in \mathbb{N}$ , and denote by  $\pi_c$  the stationary distribution of  $(\theta_{(t)}^{(0)}, \theta_t^{(1)})$ . For any  $\epsilon \in (0, 1)$ , the  $\epsilon$ -mixing times of the two algorithms are respectively defined as

$$t_{\text{mix,d}}(\epsilon) := \min \{t \in \mathbb{N} : \|P_d^t - \pi_d\|_{\text{TV}} \leq \epsilon\}, \quad t_{\text{mix,c}}(\epsilon) := \min \{t \in \mathbb{N} : \|P_c^t - \pi_c\|_{\text{TV}} \leq \epsilon\},$$

where  $\|\cdot\|_{\text{TV}}$  is the total variation distance. Theorems 3.3 and 3.4 below establish explicit mixing time upper bounds for both algorithms.

**Theorem 3.3.** *Assume that  $\max_{i \in [B]} L(\theta_i^{(0)}|\mathbf{X}) \in (0, \infty)$ . For any  $\epsilon \in (0, 1)$ , we have*

$$t_{\text{mix,d}}(\epsilon) \leq \left\lceil \frac{\max_{i \in [B]} L(\theta_i^{(0)}|\mathbf{X})}{\rho B^{-1} \sum_{i=1}^B L(\theta_i^{(0)}|\mathbf{X})} \log(\epsilon^{-1}) \right\rceil.$$

**Theorem 3.4.** *Recall the definition of  $\hat{\pi}_{\text{KDE}}(\theta)$  from (2). Assume that  $\sup_{\theta \in \mathbb{R}^d} L(\theta|\mathbf{X}) < \infty$  and  $\int_{\mathbb{R}^d} \hat{\pi}_{\text{KDE}}(\theta)L(\theta|\mathbf{X})d\theta > 0$ . For any  $\epsilon \in (0, 1)$ , we have*

$$t_{\text{mix,c}}(\epsilon) \leq \left\lceil \frac{\sup_{\theta \in \mathbb{R}^d} L(\theta|\mathbf{X})}{\rho \int_{\mathbb{R}^d} \hat{\pi}_{\text{KDE}}(\theta)L(\theta|\mathbf{X})d\theta} \log(\epsilon^{-1}) \right\rceil.$$

In view of the analysis in Section 3.1, when  $B \rightarrow \infty$  and  $h \rightarrow 0$  such that  $Bh^d \rightarrow \infty$ , the mixing time upper bound in Theorem 3.4 is upper bounded by

$$\frac{\sup_{\theta \in \mathbb{R}^d} L(\theta|\mathbf{X})}{\rho \int_{\mathbb{R}^d} \pi(\theta) L(\theta|\mathbf{X}) d\theta} \log(\epsilon^{-1}) + 2 \quad (10)$$

with high probability. When  $B \rightarrow \infty$ , the same conclusion holds for the mixing time upper bound in Theorem 3.3. Note that (10) is *independent of  $B$  and  $h$* , which implies rapid mixing of both algorithms in many practical scenarios. We will further illustrate this point numerically in Section 4.5.

The proofs of Theorems 3.3 and 3.4 are based on the Doeblin condition. We present the proof of Theorem 3.4 below, and defer the proof of Theorem 3.3 to Section A.2 of the supplementary material.

*Proof of Theorem 3.4.* We denote by  $P_c(\cdot, \cdot)$  the transition kernel of the Markov chain  $(\theta_{(t)}^{(0)}, \theta_t^{(1)})$ ,  $t \in \mathbb{N}$  in the graph-enabled MCMC. For any  $\theta_i^{(0)}, \theta_j^{(0)} \in \Theta_0$  (where  $i, j \in [B]$ ),  $\theta \in \mathbb{R}^d$ , and Borel measurable set  $A \subseteq \mathbb{R}^d$ ,

$$\begin{aligned} & P_c((\theta_i^{(0)}, \theta), \{\theta_j^{(0)}\} \times A) \\ & \geq \int_A \left( \frac{\rho}{B} + \frac{1-\rho}{D_k(\theta_i^{(0)})} \mathbb{1}_{\{\theta_i^{(0)}, \theta_j^{(0)}\} \in E_k} \right) \cdot \frac{1}{h^d} K \left( \frac{\theta' - \theta_j^{(0)}}{h} \right) \\ & \quad \cdot \min \left\{ \frac{\frac{\rho}{B} + \frac{1-\rho}{D_k(\theta_j^{(0)})} \mathbb{1}_{\{\theta_i^{(0)}, \theta_j^{(0)}\} \in E_k}}{\frac{\rho}{B} + \frac{1-\rho}{D_k(\theta_i^{(0)})} \mathbb{1}_{\{\theta_i^{(0)}, \theta_j^{(0)}\} \in E_k}} \cdot \frac{L(\theta'|\mathbf{X})}{L(\theta|\mathbf{X})}, 1 \right\} d\theta' \\ & = \int_A \min \left\{ \left( \frac{\rho}{B} + \frac{1-\rho}{D_k(\theta_j^{(0)})} \mathbb{1}_{\{\theta_i^{(0)}, \theta_j^{(0)}\} \in E_k} \right) \cdot \frac{L(\theta'|\mathbf{X})}{L(\theta|\mathbf{X})}, \frac{\rho}{B} + \frac{1-\rho}{D_k(\theta_i^{(0)})} \mathbb{1}_{\{\theta_i^{(0)}, \theta_j^{(0)}\} \in E_k} \right\} \\ & \quad \cdot \frac{1}{h^d} K \left( \frac{\theta' - \theta_j^{(0)}}{h} \right) d\theta' \geq \frac{\rho}{Bh^d} \int_A K \left( \frac{\theta' - \theta_j^{(0)}}{h} \right) \min \left\{ \frac{L(\theta'|\mathbf{X})}{L(\theta|\mathbf{X})}, 1 \right\} d\theta'. \end{aligned}$$

By the proof of Proposition 2.2,

$$\pi_c(\{\theta_j^{(0)}\} \times A) = \frac{\int_A \frac{1}{h^d} K \left( \frac{\theta' - \theta_j^{(0)}}{h} \right) L(\theta'|\mathbf{X}) d\theta'}{\sum_{\ell=1}^B \int_{\mathbb{R}^d} \frac{1}{h^d} K \left( \frac{\gamma - \theta_\ell^{(0)}}{h} \right) L(\gamma|\mathbf{X}) d\gamma} = \frac{\frac{1}{Bh^d} \int_A K \left( \frac{\theta' - \theta_j^{(0)}}{h} \right) L(\theta'|\mathbf{X}) d\theta'}{\int_{\mathbb{R}^d} \hat{\pi}_{\text{KDE}}(\gamma) L(\gamma|\mathbf{X}) d\gamma}.$$

Hence for any  $i, j \in [B]$ ,  $\theta \in \mathbb{R}^d$ , and Borel measurable set  $A \subseteq \mathbb{R}^d$ ,

$$P_c((\theta_i^{(0)}, \theta), \{\theta_j^{(0)}\} \times A) \geq \frac{\rho \int_{\mathbb{R}^d} \hat{\pi}_{\text{KDE}}(\gamma) L(\gamma|\mathbf{X}) d\gamma}{\sup_{\gamma \in \mathbb{R}^d} L(\gamma|\mathbf{X})} \pi_c(\{\theta_j^{(0)}\} \times A).$$

By this Doeblin condition (see e.g. Rosenthal (1995)),

$$\|P_c^t - \pi_c\|_{\text{TV}} \leq \left(1 - \frac{\rho \int_{\mathbb{R}^d} \hat{\pi}_{\text{KDE}}(\theta) L(\theta|\mathbf{X}) d\theta}{\sup_{\theta \in \mathbb{R}^d} L(\theta|\mathbf{X})}\right)^t, \quad \forall t \in \mathbb{N},$$

from which the conclusion of the theorem follows. □

### 3.3 Computational complexity and comparison with the Metropolis random walk

In this subsection, we analyze the computational complexity of the graph-enabled MCMC algorithm and compare it with the Metropolis random walk with Gaussian proposal.

For both versions of the graph-enabled MCMC algorithm, the construction of the graph at the beginning requires order  $B^2$  distance evaluations. After constructing the graph, running one iteration of the Markov chain requires 2 likelihood evaluations and does not require any kernel evaluation. In contrast, the Metropolis random walk with Gaussian proposal requires 2 likelihood evaluations and  $2B$  kernel evaluations (note that the computational cost for one kernel evaluation grows with the dimension  $d$ ) for each iteration. Therefore, when  $B$  or  $d$  is large, the graph-enabled MCMC algorithm requires substantially less amount of computation than the Metropolis random walk for each iteration. In Section 4.6, we further demonstrate this point numerically.

## 4 Numerical experiments

In this section, we evaluate the empirical performance of the graph-enabled MCMC (Algorithm II) introduced in Section 2 through two numerical experiments. The first experiment is an illustrative example on posterior inference with Gaussian mixture prior distribution when the exact prior distribution is unknown. The second experiment focuses on posterior inference on synthetic data sets motivated by the OUD study in Section 1.1.

### 4.1 Experimental setup

In this subsection, we describe the setup of the two numerical experiments.

#### 4.1.1 Experiment I

The first experiment (referred to as “Experiment I” hereafter) focuses on posterior inference with Gaussian mixture prior distribution. Let  $\sigma, \tau > 0$  and  $\mu_1, \mu_2, \mu_3 \in \mathbb{R}^d$ , where  $d$  is the dimension of the parameter. We assume that the true parameter  $\theta \in \mathbb{R}^d$  is drawn from a Gaussian mixture prior  $\frac{1}{3} \sum_{k=1}^3 \mathcal{N}(\mu_k, \sigma^2 I_d)$ . Given  $\theta$ , the observations  $X_1, X_2, \dots, X_n$  are drawn i.i.d. from  $\mathcal{N}(\theta, \tau^2 I_d)$ . We denote  $\mathbf{X} := (X_1, \dots, X_n)$  hereafter. Besides the observations  $\mathbf{X}$ , we also assume that  $B$  draws from the prior distribution – denoted by  $\theta_1^{(0)}, \theta_2^{(0)}, \dots, \theta_B^{(0)}$  – are available to us. Our aim is to perform posterior inference based on the observations and the prior samples, without knowing the true prior distribution (in particular, we know the value of  $\tau$  but do not know the values of  $\sigma, \mu_1, \mu_2, \mu_3$ ).

In the numerical simulations, we take  $d = 2$ ,  $\sigma = 1$ ,  $\tau = 2$ ,  $\mu_1 = (4, 0)$ ,  $\mu_2 = (-4, 0)$ ,  $\mu_3 = (0, 4)$ ,  $B = 100$ , and  $n = 10$ .

### 4.1.2 Experiment II

The second experiment (referred to as “Experiment II” hereafter) concerns synthetic OUD data sets inspired by the case study in Section 1.1. The concrete setup can be described as follows. Let  $\mu_0, \mu_1, \mu_2 \in \mathbb{R}^d$  and let  $\Sigma_0, \Sigma_1, \Sigma_2$  be  $d \times d$  positive definite matrices. We denote by  $\beta \in \mathbb{R}^d$  the parameter. We assume the following statistical model for the two populations of individuals with untreated OUD from the states of Ohio and New York:

- **Population 1 (Ohio data):** The observations are  $\{(\mathbf{x}_i, y_i)\}_{i=1}^m$ , where  $\mathbf{x}_i \in \mathbb{R}^d$  denotes the characteristics of the  $i$ th individual from Ohio and  $y_i \in \{0, 1\}$  indicates whether that individual dies ( $y_i = 1$ ) or not ( $y_i = 0$ ). For each  $i \in [m]$ , we assume that  $\mathbf{x}_i \sim \mathcal{N}(\mu_1, \Sigma_1)$  and  $y_i | \mathbf{x}_i \sim \text{Bernoulli}\left(\frac{e^{\mathbf{x}_i^\top \beta}}{1 + e^{\mathbf{x}_i^\top \beta}}\right)$ . We denote  $\mathbf{X} := \{\mathbf{x}_i\}_{i=1}^m$  and  $\mathbf{y} := \{y_i\}_{i=1}^m$ .
- **Population 2 (New York data):** The observations are  $\{(\tilde{\mathbf{x}}_i, \tilde{y}_i)\}_{i=1}^n$ , where  $\tilde{\mathbf{x}}_i \in \mathbb{R}^d$  represents the characteristics of the  $i$ th individual from New York and  $\tilde{y}_i \in \{0, 1\}$  is an indicator variable interpreted similarly as in Population 1. For each  $i \in [n]$ , we assume that  $\tilde{\mathbf{x}}_i \sim \mathcal{N}(\mu_2, \Sigma_2)$  and  $\tilde{y}_i | \tilde{\mathbf{x}}_i \sim \text{Bernoulli}\left(\frac{e^{\tilde{\mathbf{x}}_i^\top \beta}}{1 + e^{\tilde{\mathbf{x}}_i^\top \beta}}\right)$ . We denote  $\tilde{\mathbf{X}} := \{\tilde{\mathbf{x}}_i\}_{i=1}^n$  and  $\tilde{\mathbf{y}} := \{\tilde{y}_i\}_{i=1}^n$ .

We assume a Gaussian prior for the parameter:  $\beta \sim \mathcal{N}(\mu_0, \Sigma_0)$ . Given  $\beta$ , the observations from the two populations are independently generated as above. We note the potential shift in the covariate distributions ( $\mathcal{N}(\mu_1, \Sigma_1)$  and  $\mathcal{N}(\mu_2, \Sigma_2)$ ) between the two populations.

As discussed in Section 1.1, the reference study is based on a Bayesian analysis of the data  $(\mathbf{X}, \mathbf{y})$  from Ohio. For any  $\mu \in \mathbb{R}^d$  and  $d \times d$  positive definite matrix  $\Sigma$ , we denote by  $\phi_{\mu, \Sigma}(\cdot)$  the density of  $\mathcal{N}(\mu, \Sigma)$ . The posterior distribution of  $\beta$  in the reference study is

$$\pi(\beta | \mathbf{X}, \mathbf{y}) \propto \phi_{\mu_0, \Sigma_0}(\beta) \prod_{i=1}^m \frac{e^{y_i \mathbf{x}_i^\top \beta}}{1 + e^{\mathbf{x}_i^\top \beta}}.$$

We assume that  $B = 10000$  samples  $\beta_1^{(0)}, \dots, \beta_B^{(0)}$  from the posterior  $\pi(\beta|\mathbf{X}, \mathbf{y})$  are generated using MCMC (in our implementation, we use the `rjags` R package to generate the MCMC samples; we run 40000 iterations and drop the first 30000 samples as burn-in). As mentioned in Section 1.1, due to data availability and sharing issues, only these posterior samples are available to us from the reference study.

For the current study, we focus on the posterior distribution of  $\beta$  using the data  $(\tilde{\mathbf{X}}, \tilde{\mathbf{y}})$  from New York. There are two choices for the prior distribution: the *uninformative prior*  $\mathcal{N}(\mu_0, \Sigma_0)$ , or the *informative prior*  $\pi(\beta|\mathbf{X}, \mathbf{y})$  based on the reference study. The informative prior results in a posterior that integrates the information from the reference study into the current study. In this numerical experiment, we aim to generate samples from the posterior distribution in the current study with informative prior. For comparison, we also generate samples from the posterior distribution in the current study with uninformative prior (implemented similarly to the reference study).

In the numerical simulations, we consider a range of dimensions  $d \in \{2, 6, 10\}$ . We fix the other model parameters as  $m = n = 1500$ ,  $\mu_0 = (0, \dots, 0)$ ,  $\mu_1 = (1, \dots, 1)$ ,  $\mu_2 = (-1, \dots, -1)$ , and  $\Sigma_0 = \Sigma_1 = \Sigma_2 = I_d$ .

## 4.2 Comparison methods

In the numerical experiments, we compare the performance of the graph-enabled MCMC with two alternative approaches. The first one, which we term ‘‘Gaussian MCMC’’, estimates the prior distribution by fitting a Gaussian distribution to the prior samples and draws MCMC samples from the resulting approximate posterior. The second one is the Metropolis random walk with Gaussian proposal described in Section 1.2.

We describe the algorithm parameters for the graph-enabled MCMC and the Metropolis

random walk in the two numerical experiments as follows. For both experiments, we use the Gaussian kernel (4). In Experiment I, for the graph-enabled MCMC, we take  $k = 10$ ,  $\rho = 0.5$ , and  $h = 1$ ; for the Metropolis random walk, we take  $\sigma_p = 0.5$  and  $h = 1$ . In Experiment II, for the graph-enabled MCMC, we take  $k = \lceil \sqrt{B} \rceil$ ,  $\rho = 0.5$ , and  $h = 0.04$ ; for the Metropolis random walk, we take  $\sigma_p = 0.02$  and  $h = 0.04$ . For both experiments, we run each algorithm for 10000 iterations (dropping the first 5000 samples as burn-in) and replicate for three times.

### 4.3 Evaluation metrics

In this subsection, we briefly describe the metrics that we use to evaluate the performance of the graph-enabled MCMC and the alternative approaches discussed in Section 4.2. We evaluate the performance of these algorithms in terms of the following three aspects: (1) validity of posterior approximation; (2) mixing and statistical efficiency; (3) computational complexity. The results on these aspects will be presented in Sections 4.4-4.6, respectively.

To assess the validity of the estimated posteriors constructed via MCMC samples, in addition to the contour plots presented in Figures 1 and 2, we present the 2-Wasserstein distance between the true and estimated posteriors (see e.g. (Villani, 2009, Chapter 6) for background on the 2-Wasserstein distance). To examine the mixing behavior of MCMC algorithms, we display several MCMC convergence diagnostics, including traceplots, Gelman-Rubin convergence diagnostics (Gelman and Rubin (1992); Brooks and Gelman (1998)), and autocorrelation plots; to examine the statistical efficiency, we compute the effective sample size for each algorithm. To compare the computational efficiency of the algorithms, we examine the computation time per iteration for each algorithm.

## 4.4 Results on validity of posterior approximation

In Table 1, we display the 2-Wasserstein distance between the true and estimated posteriors in Experiment I (we approximate the true posterior via samples from a Metropolis sampler using the exact prior information and average the results over 3 replications). We observe that the estimated posteriors using the graph-enabled MCMC and the Metropolis random walk both approximate the true posterior well with similar accuracy; in comparison, the estimated posterior obtained by Gaussian MCMC has a substantially larger 2-Wasserstein distance to the true posterior. Combining this with our observation from Figure 1 in the Introduction, we conclude that both the graph-enabled MCMC and the Metropolis random walk give valid approximations to the true posterior, while the approximate posterior constructed by Gaussian MCMC is not reliable. Further evidence in favor of the graph-enabled MCMC and the Metropolis random walk is presented in Figure 8 of the supplementary material, where we display contour plots and boxplots for the true and estimated posteriors.

Method	Graph-enabled MCMC	Metropolis random walk	Gaussian MCMC
2-Wasserstein distance	0.13	0.13	0.27

Table 1: 2-Wasserstein distance between the true and estimated posteriors: Experiment I

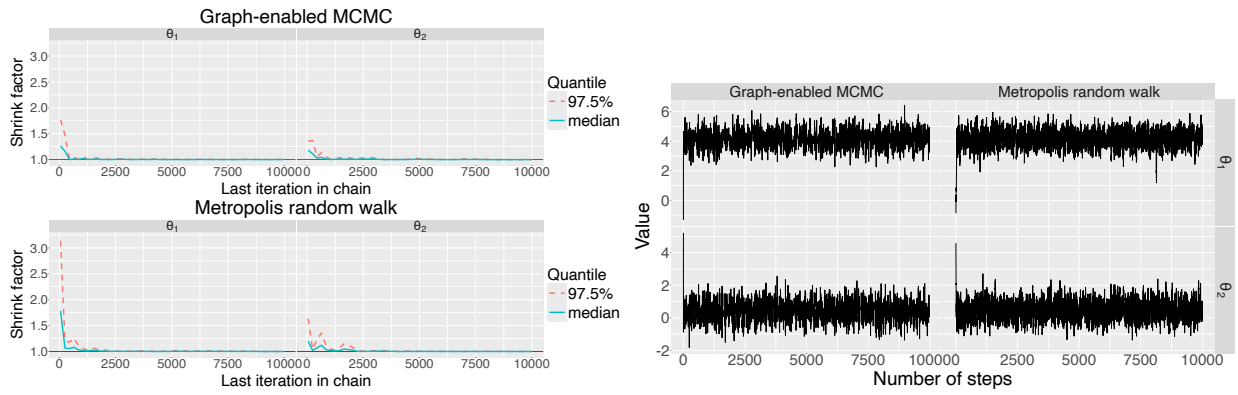
We also present the 2-Wasserstein distance between the true and estimated posteriors in Experiment II in Table 2, which again demonstrates that both the graph-enabled MCMC and the Metropolis random walk give reliable approximations to the true posterior.

Method	$d = 2$	$d = 6$	$d = 10$
Graph-enabled MCMC	0.020	0.060	0.16
Metropolis random walk	0.022	0.057	0.15

Table 2: 2-Wasserstein distance between the true and estimated posteriors: Experiment II

## 4.5 Results on mixing and statistical efficiency

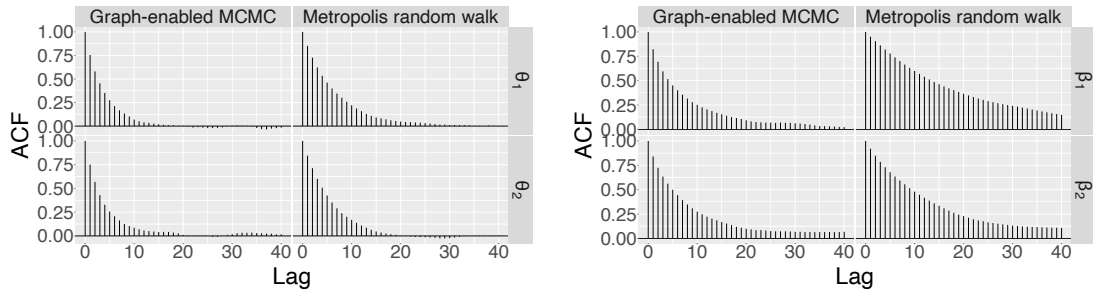
In this subsection, we display the mixing behavior and statistical efficiency of the graph-enabled MCMC and the Metropolis random walk. In Figure 3, we present the Gelman-Rubin-Brooks plots and the traceplots for Experiment I. From these plots, we observe that both algorithms mix rapidly, and their mixing rates appear to be of similar order. The corresponding plots for Experiment II are presented in the supplementary material (Figures 9-11) and exhibit similar patterns. In Figure 4, we present the autocorrelation plots for both experiments. From this figure, we observe that the graph-enabled MCMC has smaller autocorrelation than the Metropolis random walk, which indicates better mixing and statistical efficiency. In Table 3, we present the multivariate potential scale reduction factors (MPSRF; see Brooks and Gelman (1998)) and the effective sample sizes (based on the remaining 5000 samples after dropping the first 5000 samples as burn-in) for both experiments. From this table, we observe that the MPSRF for both algorithms are very close to 1, indicating that both algorithms are well-mixed after 10000 iterations; moreover, the effective sample size for the graph-enabled MCMC is substantially larger than that for the Metropolis random walk, which demonstrates the higher statistical efficiency of the graph-enabled MCMC.



(a) Gelman-Rubin-Brooks plots

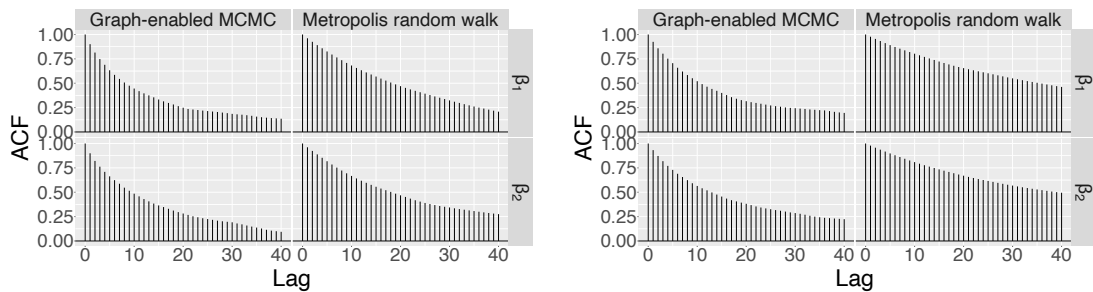
(b) Traceplots

Figure 3: MCMC convergence diagnostics in Experiment I



(a) Experiment I

(b) Experiment II:  $d = 2$



(c) Experiment II:  $d = 6$

(d) Experiment II:  $d = 10$

Figure 4: Autocorrelation plots

## 4.6 Results on computational complexity

In this subsection, we compare the computational efficiency of the graph-enabled MCMC and the Metropolis random walk. In Table 4, we present the computation time per iteration in both experiments. We observe that the graph-enabled MCMC has much less

	Method	Experiment I	Experiment II		
			$d = 2$	$d = 6$	$d = 10$
MPSRF	Graph	1.00	1.01	1.02	1.07
	Metropolis	1.00	1.00	1.04	1.06
Effective sample size for $\theta_1/\beta_1$	Graph	686	339	189	179
	Metropolis	464	121	111	56
Effective sample size for $\theta_2/\beta_2$	Graph	645	307	213	129
	Metropolis	442	172	96	51

Table 3: MPSRF and effective sample size (Graph: graph-enabled MCMC; Metropolis: Metropolis random walk): averaged over three replications

computational cost per iteration (more than 6 times faster) than the Metropolis random walk.

Method	Experiment I	Experiment II		
		$d = 2$	$d = 6$	$d = 10$
Graph-enabled MCMC	$1.37 \cdot 10^{-4}$	0.017	0.018	0.018
Metropolis random walk	$1.05 \cdot 10^{-3}$	0.11	0.11	0.11

Table 4: Computation time per iteration (unit: second): averaged over three replications

To further illustrate the dependence of the computation time of the graph-enabled MCMC and the Metropolis random walk on  $B$  (the number of prior samples), we repeat Experiment II with  $B \in \{1000, 2500, 5000, 10000, 15000, 20000\}$  and  $d = 6$  (taking  $k = \lceil \sqrt{B} \rceil$  and fixing other parameters as before). In Figure 5, we plot the computation time per iteration versus  $B$  for both algorithms. We observe that the computation time per iteration

of the Metropolis random walk grows rapidly as  $B$  increases, while that of the graph-enabled MCMC almost remains constant; for all the  $B$  values considered, the graph-enabled MCMC has a substantially smaller computational cost than the Metropolis random walk. The former observation is reminiscent of the discussion on computational complexity in Section 3.3 and makes the graph-enabled MCMC particularly desirable for practical applications (as increasingly large values of  $B$  are needed to obtain a more accurate approximation to the true posterior).

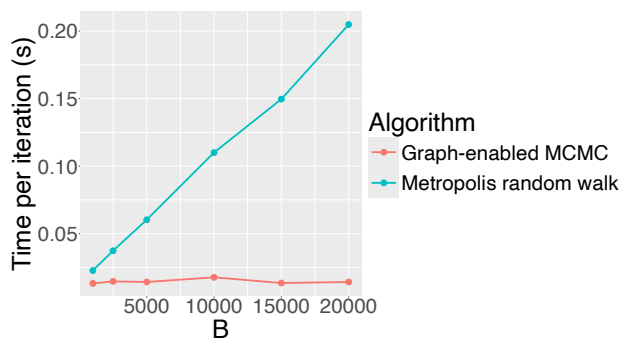


Figure 5: Computation time per iteration (unit: second) versus  $B$  in Experiment II:  $d = 6$ , averaged over three replications

Since the graph-enabled MCMC has similar or better mixing behavior and higher statistical efficiency compared to the Metropolis random walk (as demonstrated in Section 4.5), we conclude that the graph-enabled MCMC is computationally much more efficient than the Metropolis random walk.

## 5 Application to a human behavior experimental study

In this section, we discuss an application of the graph-enabled MCMC algorithm to a human behavior experimental study from the Next Generation Social Science (NGS2) program (Smith et al. (2023)). In this study, a research team led by scientists at Gallup investi-

gated the influence of social networks in a public goods game (from economic game theory; see Ledyard (1995)). In a public goods game,  $n$  players can choose whether to contribute (“cooperate”) or not (“defect”) over a total of  $T$  sequential rounds. The contribution of a player is split among the player’s neighbors in the (possibly evolving) social network. Each player is assigned to one of four conditions determining the evolution of the social network (see Smith et al. (2023) for details): (1) fixed links (the network is static); (2) random link updating (after each round, the network is regenerated randomly); (3) viscous strategic link updating (10% of subject pairs were randomly selected and a randomly selected actor of each selected pair may change the link status of the pair); (4) fluid strategic link updating (similar to (3) but with 30% of pairs selected; also referred to as “rapidly updating networks”). If player  $i$  at round  $t$  chooses to cooperate, we let  $Y_{it} = 1$ ; otherwise we let  $Y_{it} = 0$ . Following the discussions in Smith et al. (2023), such decision can be modeled as

$$Y_{it} \stackrel{ind}{\sim} \text{Bernoulli}(p_{it}), \quad \log\left(\frac{p_{it}}{1-p_{it}}\right) = \beta_1 + \beta_2 X_i + \beta_3 t + \beta_4 X_i t,$$

where  $X_i \in \{0, 1\}$  indicates whether the participant  $i$  is included in the rapidly updating network condition. In addition to this study by the Gallup team, an earlier study conducted by Rand et al. (2011) on the same scientific problem was also available to us. In the following, we treat the earlier study by Rand et al. (2011) as the reference study and the study conducted by the Gallup team as the current study. Relevant data are available at <https://github.com/gal-zz-lup/NGS2>.

For both studies, we assume the following Gaussian prior on the parameters (as used in Smith et al. (2023)):  $\beta_1 \sim \mathcal{N}(0, 2.5^2)$ ,  $\beta_2 \sim \mathcal{N}(0, 5.3^2)$ ,  $\beta_3 \sim \mathcal{N}(0, 0.8^2)$ ,  $\beta_4 \sim \mathcal{N}(0, 1)$ , where  $\beta_1, \beta_2, \beta_3, \beta_4$  are assumed to be independent. For each study, we obtain  $B = 5000$  posterior draws based on this prior and the corresponding data (using the `rjags` R package; we run 20000 iterations and drop the first 15000 samples as burn-in). In Figure 6, we

present a boxplot of the posterior draws for each of the two studies (we refer to these two posteriors as “posterior in the reference study” and “posterior in the current study with uninformative prior”). From the figure, we observe that the posterior distributions of  $\beta_1$  and  $\beta_2$  from the two studies appear to be quite different, while those of  $\beta_3$  and  $\beta_4$  are relatively close. Motivated by this observation, we would like to integrate the valuable information regarding  $\beta_3$  and  $\beta_4$  from the reference study into the current study to obtain a more informative posterior, which could also benefit downstream inference and prediction tasks. We refer to this posterior as “posterior in the current study with informative prior”. To achieve this goal, we apply the generalized graph-enabled MCMC algorithm in Section 2.4 to the two studies, treating  $\beta_3$  and  $\beta_4$  as the shared parameters and taking the algorithm parameters to be  $k = \lceil \sqrt{B} \rceil$ ,  $h = 0.01$ ,  $\sigma = 0.05$ ,  $\rho = 0.5$ . We run the algorithm for 100000 iterations and drop the first 50000 samples as burn-in.

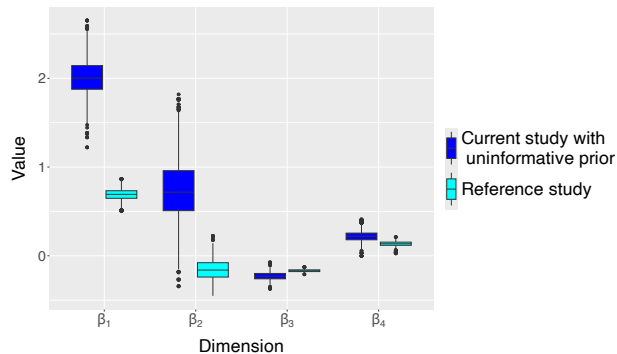


Figure 6: Boxplot of posterior draws in the reference study and the current study with uninformative prior

In Figure 7, we compare the posterior distributions in the two studies. In panel (a), we display posterior draws in the reference study as cyan dots and present contour plots for posterior draws in the current study with uninformative prior (in blue) and informative prior (in red). In panel (b), we present a boxplot of the resulting estimated posteriors.

From the figure, we observe that the posterior in the current study with informative prior interpolates between the posterior in the reference study and the posterior in the current study with uninformative prior (in particular, note the shift in posterior mode between the two contours), which indicates that the posterior in the current study with informative prior successfully integrates the information from the reference study into the current study. We also observe that the uncertainty in the posterior in the current study with informative prior is substantially smaller than that with uninformative prior (with a narrower interquartile range in the boxplot and a more concentrated contour), which further demonstrates the importance of incorporating the valuable information from the reference study into the current study.

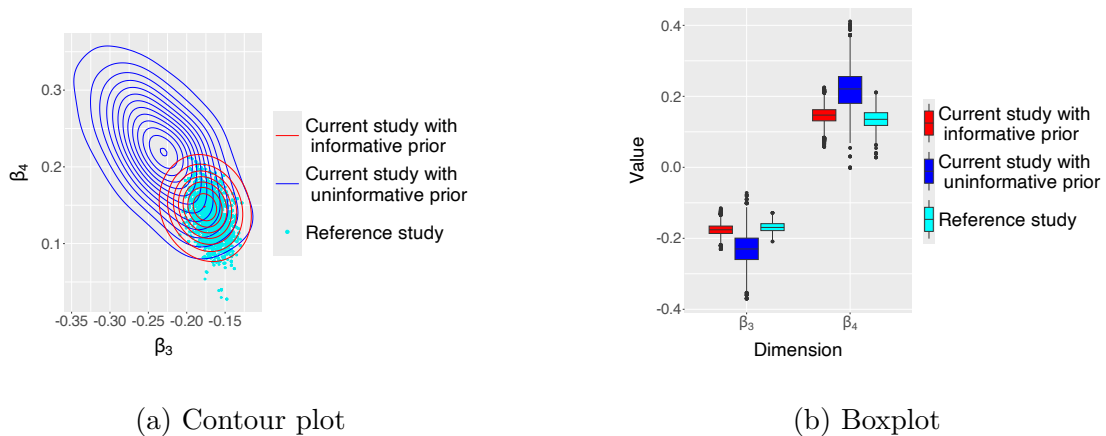


Figure 7: Comparison of posterior distributions

## 6 Discussion and conclusions

In this paper, we propose a graph-based MCMC algorithm that enables efficient sampling from the posterior distribution when the prior distribution is unknown and needs to be estimated from prior draws. The algorithm constructs a geometric graph based on prior samples and leverages the graph structure to guide the transitions of the Markov chain.

Through both theoretical and numerical studies, we show that our algorithm provides reliable approximation to the true posterior and achieves substantially better computational performance than alternative approaches.

In the following, we discuss an adaptation of the graph-enabled MCMC algorithm for handling prior-likelihood distributional gaps. We expect this extension to further improve the practical performance of our algorithm, and plan to report on its applications in future works.

**Adaptive algorithm for prior-likelihood distributional gaps.** In practice, there can be situations where the prior distribution and the likelihood function have almost disjoint support. For example, this happens when the data generating mechanisms underlying the pilot study and the realized experiment are substantially different. In such scenarios, it is desirable to focus more on the likelihood function representing the current data. Here, we propose an adaptive version of the graph-enabled MCMC algorithm that improves on the robustness of the algorithm under such regimes.

We fix  $\gamma \in (0, 1)$ ,  $\epsilon > 0$ , and introduce the weakly informative prior distribution

$$\hat{\pi}_{\gamma, \epsilon}(\theta) \propto \frac{\gamma}{Bh^d} \sum_{i=1}^B K\left(\frac{\theta - \theta_i^{(0)}}{h}\right) + (1 - \gamma)\epsilon. \quad (11)$$

Note that  $\hat{\pi}_{\gamma, \epsilon}(\cdot)$  is a linear combination of the kernel density estimate of the prior distribution and the uninformative prior  $\pi_0(\theta) \propto \epsilon$ . Using  $\hat{\pi}_{\gamma, \epsilon}(\cdot)$  to approximate the true prior distribution, we obtain the following approximate posterior distribution:

$$\begin{aligned} \hat{\pi}_{\gamma, \epsilon}(\theta|\mathbf{X}) &\propto \left( \frac{\gamma}{Bh^d} \sum_{i=1}^B K\left(\frac{\theta - \theta_i^{(0)}}{h}\right) + (1 - \gamma)\epsilon \right) L(\theta|\mathbf{X}) \\ &= \sum_{i=1}^B \frac{\gamma}{Bh^d} K\left(\frac{\theta - \theta_i^{(0)}}{h}\right) L(\theta|\mathbf{X}) + (1 - \gamma)\epsilon L(\theta|\mathbf{X}). \end{aligned} \quad (12)$$

We assume  $\int_{\mathbb{R}^d} L(\theta|\mathbf{X})d\theta < \infty$ . To sample from (12), we augment the set  $\Theta_0$  with a distinguished element  $\Delta$  to form  $\tilde{\Theta}_0 := \Theta_0 \cup \{\Delta\}$ , and construct the graph  $G_k$  with vertex

set  $\Theta_0$  as in Section 2.2. We aim to jointly sample  $(\alpha, \theta) \in \tilde{\Theta}_0 \times \mathbb{R}^d$  from the density

$$\Phi_{\gamma, \epsilon}(\alpha, \theta) = \begin{cases} Z_{\gamma, \epsilon}^{-1} (1 - \gamma) \epsilon L(\theta | \mathbf{X}) & \text{if } \alpha = \Delta \\ Z_{\gamma, \epsilon}^{-1} \frac{\gamma}{B h^d} K\left(\frac{\theta - \alpha}{h}\right) L(\theta | \mathbf{X}) & \text{if } \alpha \in \Theta_0 \end{cases} \quad (13)$$

with respect to the product of the counting measure on  $\tilde{\Theta}_0$  and the Lebesgue measure on  $\mathbb{R}^d$ , where  $Z_{\gamma, \epsilon}$  is the normalizing constant. Note that the marginal density of  $\theta$  under the joint density  $\Phi_{\gamma, \epsilon}(\cdot, \cdot)$  is exactly the approximate posterior (12). We have developed an adaptation of the graph-enabled MCMC for sampling from (13) (and hence from (12)). The details of this algorithm are presented in Section C of the supplementary material.

## SUPPLEMENTARY MATERIAL

The code for reproducing numerical results in this paper is available at <https://github.com/cyzhong17/Graph-Enabled-MCMC>. In the supplementary material, we present the proofs of Theorems 3.2 and 3.3, additional figures from the numerical experiments in Section 4, and the details of the adaptive algorithm for handling prior-likelihood distributional gaps discussed in Section 6.

## References

- Blanco, C. and N. D. Volkow (2019). Management of opioid use disorder in the USA: present status and future directions. *The Lancet* 393(10182), 1760–1772.
- Borenstein, M., L. V. Hedges, J. P. Higgins, and H. R. Rothstein (2021). *Introduction to meta-analysis*. John Wiley & Sons.
- Brooks, S., A. Gelman, G. Jones, and X.-L. Meng (2011). *Handbook of Markov chain Monte Carlo*. CRC press.

- Brooks, S. P. and A. Gelman (1998). General methods for monitoring convergence of iterative simulations. *Journal of computational and graphical statistics* 7(4), 434–455.
- Chandra, R. and A. Kapoor (2020). Bayesian neural multi-source transfer learning. *Neurocomputing* 378, 54–64.
- Devroye, L. and G. Lugosi (2001). *Combinatorial methods in density estimation*. Springer Science & Business Media.
- Diaconis, P. and L. Saloff-Coste (1995). What do we know about the Metropolis algorithm? In *Proceedings of the twenty-seventh annual ACM symposium on Theory of computing*, pp. 112–129.
- Doogan, N. J., A. Mack, J. Wang, D. Crane, R. Jackson, M. Applegate, J. Villani, R. Chandler, and J. A. Barocas (2022). Opioid use disorder among Ohio’s medicaid population: Prevalence estimates from 19 counties using a multiplier method. *American Journal of Epidemiology* 191(12), 2098–2108.
- Gelman, A. and D. B. Rubin (1992). Inference from iterative simulation using multiple sequences. *Statistical science* 7(4), 457–472.
- Gönen, M. and A. Margolin (2014). Kernelized Bayesian transfer learning. In *Proceedings of the AAAI Conference on Artificial Intelligence*, Volume 28.
- Gramacki, A. (2018). *Nonparametric kernel density estimation and its computational aspects*, Volume 37. Springer.
- Karbalayghareh, A., X. Qian, and E. R. Dougherty (2018). Optimal Bayesian transfer learning. *IEEE Transactions on Signal Processing* 66(14), 3724–3739.

- Kim, N. J., B. R. Belland, and A. E. Walker (2018). Effectiveness of computer-based scaffolding in the context of problem-based learning for STEM education: Bayesian meta-analysis. *Educational Psychology Review* 30, 397–429.
- Ledyard, O. (1995). Public goods: some experimental results. *Handbook of experimental economics* 1.
- Levin, D. A. and Y. Peres (2017). *Markov chains and mixing times*, Volume 107. American Mathematical Soc.
- Liu, J. S. and J. S. Liu (2001). *Monte Carlo strategies in scientific computing*, Volume 10. Springer.
- Metropolis, N., A. W. Rosenbluth, M. N. Rosenbluth, A. H. Teller, and E. Teller (1953). Equation of state calculations by fast computing machines. *The journal of chemical physics* 21(6), 1087–1092.
- Parzen, E. (1962). On estimation of a probability density function and mode. *The Annals of Mathematical Statistics* 33(3), 1065–1076.
- Rand, D. G., S. Arbesman, and N. A. Christakis (2011). Dynamic social networks promote cooperation in experiments with humans. *Proceedings of the National Academy of Sciences* 108(48), 19193–19198.
- Rosenblatt, M. (1956). Remarks on some nonparametric estimates of a density function. *The Annals of Mathematical Statistics* 27(3), 832–837.
- Rosenthal, J. S. (1995). Minorization conditions and convergence rates for Markov chain Monte Carlo. *Journal of the American Statistical Association* 90(430), 558–566.

- Schmid, C. H. and K. Mengersen (2013). Bayesian meta-analysis. *The handbook of meta-analysis in ecology and evolution*, 145–173.
- Shahbaba, B., S. Lan, W. O. Johnson, and R. M. Neal (2014). Split Hamiltonian Monte Carlo. *Statistics and Computing* 24, 339–349.
- Shwartz-Ziv, R., M. Goldblum, H. Souri, S. Kapoor, C. Zhu, Y. LeCun, and A. G. Wilson (2022). Pre-train your loss: Easy Bayesian transfer learning with informative priors. *Advances in Neural Information Processing Systems* 35, 27706–27715.
- Smith, A. L., T. Zheng, and A. Gelman (2023). Prediction scoring of data-driven discoveries for reproducible research. *Statistics and Computing* 33(1), 11.
- Strang, J., N. D. Volkow, L. Degenhardt, M. Hickman, K. Johnson, G. F. Koob, B. D. Marshall, M. Tyndall, and S. L. Walsh (2020). Opioid use disorder. *Nature reviews Disease primers* 6(1), 3.
- Suder, P. M., J. Xu, and D. B. Dunson (2023). Bayesian transfer learning. *arXiv preprint arXiv:2312.13484*.
- Villani, C. (2009). *Optimal transport: old and new*, Volume 338. Springer.
- Wurpts, I. C., M. Miočević, and D. P. MacKinnon (2021). Sequential Bayesian data synthesis for mediation and regression analysis. *Prevention Science*, 1–12.
- Xuan, J., J. Lu, and G. Zhang (2021). Bayesian transfer learning: An overview of probabilistic graphical models for transfer learning. *arXiv preprint arXiv:2109.13233*.
- Zreik, T. G., A. Mazloom, Y. Chen, M. Vannucci, C. C. Pinnix, S. Fulton, M. Hadziahmetovic, N. Asmar, A. R. Munkarah, C. M. Ayoub, et al. (2010). Fertility drugs and the risk

of breast cancer: a meta-analysis and review. *Breast cancer research and treatment* 124,  
13-26.

# Supplementary Material

## A Proofs of Theorems 3.2 and 3.3

We present the proofs of Theorems 3.2 and 3.3 in Sections A.1 and A.2, respectively.

### A.1 Proof of Theorem 3.2

We note that

$$\begin{aligned}
|\tilde{\pi}(\theta|\mathbf{X}) - \hat{\pi}(\theta|\mathbf{X})| &= \left| \frac{\sum_{i=1}^B K\left(\frac{\theta - \theta_i^{(0)}}{h}\right) L(\theta_i^{(0)}|\mathbf{X})}{h^d \sum_{i=1}^B L(\theta_i^{(0)}|\mathbf{X})} - \frac{\sum_{i=1}^B K\left(\frac{\theta - \theta_i^{(0)}}{h}\right) L(\theta|\mathbf{X})}{\sum_{i=1}^B \int_{\mathbb{R}^d} K\left(\frac{\tau - \theta_i^{(0)}}{h}\right) L(\tau|\mathbf{X}) d\tau} \right| \\
&\leq \left| \frac{\sum_{i=1}^B K\left(\frac{\theta - \theta_i^{(0)}}{h}\right) L(\theta|\mathbf{X})}{h^d \sum_{i=1}^B L(\theta_i^{(0)}|\mathbf{X})} - \frac{\sum_{i=1}^B K\left(\frac{\theta - \theta_i^{(0)}}{h}\right) L(\theta|\mathbf{X})}{\sum_{i=1}^B \int_{\mathbb{R}^d} K\left(\frac{\tau - \theta_i^{(0)}}{h}\right) L(\tau|\mathbf{X}) d\tau} \right| \\
&\quad + \left| \frac{\sum_{i=1}^B K\left(\frac{\theta - \theta_i^{(0)}}{h}\right) L(\theta_i^{(0)}|\mathbf{X})}{h^d \sum_{i=1}^B L(\theta_i^{(0)}|\mathbf{X})} - \frac{\sum_{i=1}^B K\left(\frac{\theta - \theta_i^{(0)}}{h}\right) L(\theta|\mathbf{X})}{h^d \sum_{i=1}^B L(\theta_i^{(0)}|\mathbf{X})} \right| \\
&\leq \frac{\left(\sum_{i=1}^B K\left(\frac{\theta - \theta_i^{(0)}}{h}\right) L(\theta|\mathbf{X})\right) \left(\sum_{i=1}^B \int_{\mathbb{R}^d} K\left(\frac{\tau - \theta_i^{(0)}}{h}\right) |L(\tau|\mathbf{X}) - L(\theta_i^{(0)}|\mathbf{X})| d\tau\right)}{h^d \left(\sum_{i=1}^B L(\theta_i^{(0)}|\mathbf{X})\right) \left(\sum_{i=1}^B \int_{\mathbb{R}^d} K\left(\frac{\tau - \theta_i^{(0)}}{h}\right) L(\tau|\mathbf{X}) d\tau\right)} \\
&\quad + \frac{\sum_{i=1}^B K\left(\frac{\theta - \theta_i^{(0)}}{h}\right) |L(\theta_i^{(0)}|\mathbf{X}) - L(\theta|\mathbf{X})|}{h^d \sum_{i=1}^B L(\theta_i^{(0)}|\mathbf{X})} \\
&\leq \frac{M \left(\sum_{i=1}^B K\left(\frac{\theta - \theta_i^{(0)}}{h}\right) L(\theta|\mathbf{X})\right) \left(\sum_{i=1}^B \int_{\mathbb{R}^d} K\left(\frac{\tau - \theta_i^{(0)}}{h}\right) \|\tau - \theta_i^{(0)}\|_2 d\tau\right)}{h^d \left(\sum_{i=1}^B L(\theta_i^{(0)}|\mathbf{X})\right) \left(\sum_{i=1}^B \int_{\mathbb{R}^d} K\left(\frac{\tau - \theta_i^{(0)}}{h}\right) L(\tau|\mathbf{X}) d\tau\right)} \\
&\quad + \frac{M \sum_{i=1}^B K\left(\frac{\theta - \theta_i^{(0)}}{h}\right) \|\theta - \theta_i^{(0)}\|_2}{h^d \sum_{i=1}^B L(\theta_i^{(0)}|\mathbf{X})}.
\end{aligned}$$

Hence

$$\begin{aligned} \int_{\mathbb{R}^d} |\tilde{\pi}(\theta|\mathbf{X}) - \hat{\pi}(\theta|\mathbf{X})| d\theta &\leq \frac{2M \sum_{i=1}^B \int_{\mathbb{R}^d} K\left(\frac{\theta - \theta_i^{(0)}}{h}\right) \|\theta - \theta_i^{(0)}\|_2 d\theta}{h^d \sum_{i=1}^B L(\theta_i^{(0)}|\mathbf{X})} \\ &= \frac{2Mh \int_{\mathbb{R}^d} K(u) \|u\|_2 du}{B^{-1} \sum_{i=1}^B L(\theta_i^{(0)}|\mathbf{X})}. \end{aligned}$$

By the law of large numbers,  $B^{-1} \sum_{i=1}^B L(\theta_i^{(0)}|\mathbf{X}) \xrightarrow{P} \int_{\mathbb{R}^d} \pi(\theta) L(\theta|\mathbf{X}) d\theta \in (0, \infty)$  as  $B \rightarrow \infty$ .

As  $h \rightarrow 0$ , we conclude that

$$\int_{\mathbb{R}^d} |\tilde{\pi}(\theta|\mathbf{X}) - \hat{\pi}(\theta|\mathbf{X})| d\theta \xrightarrow{P} 0.$$

## A.2 Proof of Theorem 3.3

We denote by  $P_d(\cdot, \cdot)$  the transition matrix of the Markov chain  $\theta_{(t)}^{(0)}, t \in \mathbb{N}$  in the graph-enabled discretized MCMC. For any  $\theta_i^{(0)}, \theta_j^{(0)} \in \Theta_0$  (where  $i, j \in [B]$ ),

$$\begin{aligned} &P_d(\theta_i^{(0)}, \theta_j^{(0)}) \\ &\geq \left( \frac{\rho}{B} + \frac{1-\rho}{D_k(\theta_i^{(0)})} \mathbb{1}_{\{\theta_i^{(0)}, \theta_j^{(0)}\} \in E_k} \right) \min \left\{ \frac{\frac{\rho}{B} + \frac{1-\rho}{D_k(\theta_j^{(0)})} \mathbb{1}_{\{\theta_i^{(0)}, \theta_j^{(0)}\} \in E_k}}{\frac{\rho}{B} + \frac{1-\rho}{D_k(\theta_i^{(0)})} \mathbb{1}_{\{\theta_i^{(0)}, \theta_j^{(0)}\} \in E_k}} \cdot \frac{L(\theta_j^{(0)}|\mathbf{X})}{L(\theta_i^{(0)}|\mathbf{X})}, 1 \right\} \\ &= \min \left\{ \left( \frac{\rho}{B} + \frac{1-\rho}{D_k(\theta_j^{(0)})} \mathbb{1}_{\{\theta_i^{(0)}, \theta_j^{(0)}\} \in E_k} \right) \cdot \frac{L(\theta_j^{(0)}|\mathbf{X})}{L(\theta_i^{(0)}|\mathbf{X})}, \frac{\rho}{B} + \frac{1-\rho}{D_k(\theta_i^{(0)})} \mathbb{1}_{\{\theta_i^{(0)}, \theta_j^{(0)}\} \in E_k} \right\} \\ &\geq \frac{\rho}{B} \min \left\{ \frac{L(\theta_j^{(0)}|\mathbf{X})}{L(\theta_i^{(0)}|\mathbf{X})}, 1 \right\}. \end{aligned}$$

By the proof of Proposition 2.1,

$$\pi_d(\theta_j^{(0)}) = \frac{L(\theta_j^{(0)}|\mathbf{X})}{\sum_{\ell=1}^B L(\theta_\ell^{(0)}|\mathbf{X})}.$$

Hence

$$P_d(\theta_i^{(0)}, \theta_j^{(0)}) \geq \frac{\rho}{B} \cdot \frac{\sum_{\ell=1}^B L(\theta_\ell^{(0)}|\mathbf{X})}{\max_{\ell \in [B]} L(\theta_\ell^{(0)}|\mathbf{X})} \pi_d(\theta_j^{(0)}), \quad \forall i, j \in [B].$$

By this Doeblin condition,

$$\|P_d^t - \pi_d\|_{\text{TV}} \leq \left( 1 - \frac{\rho}{B} \cdot \frac{\sum_{\ell=1}^B L(\theta_\ell^{(0)}|\mathbf{X})}{\max_{\ell \in [B]} L(\theta_\ell^{(0)}|\mathbf{X})} \right)^t, \quad \forall t \in \mathbb{N},$$

from which the conclusion of the theorem follows.

## B Additional figures from the numerical experiments

In this section, we present additional figures from the numerical experiments in Section 4 of the paper. In Figure 8, we present contour plots and boxplots for the true and estimated posteriors (by the graph-enabled MCMC and the Metropolis random walk) in Experiment I, where the true posterior is approximated via samples from a Metropolis sampler using the exact prior information.

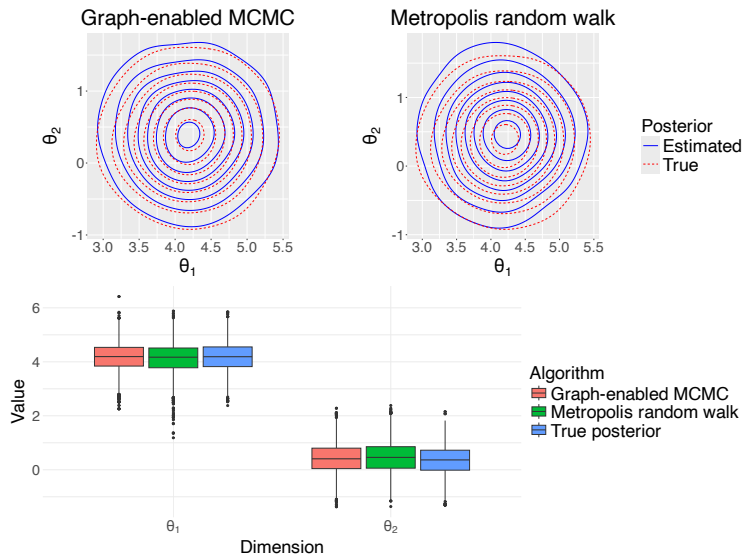
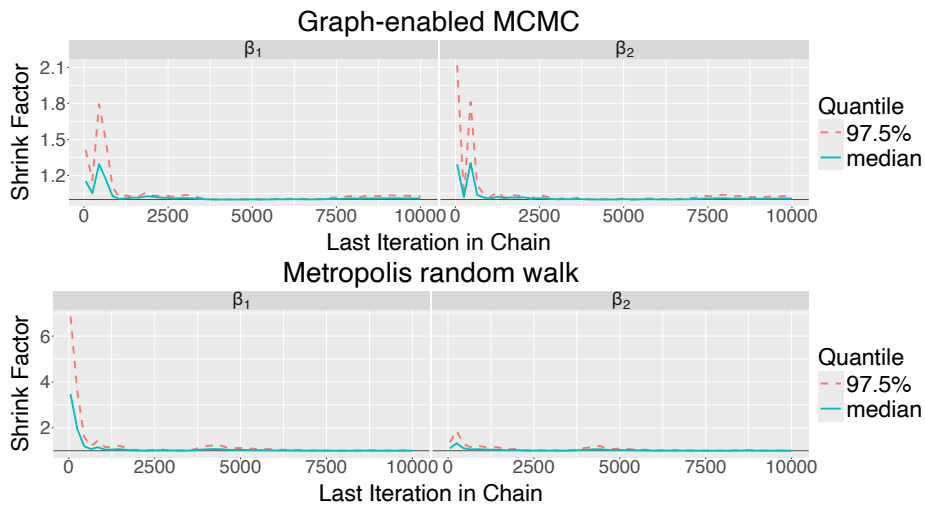
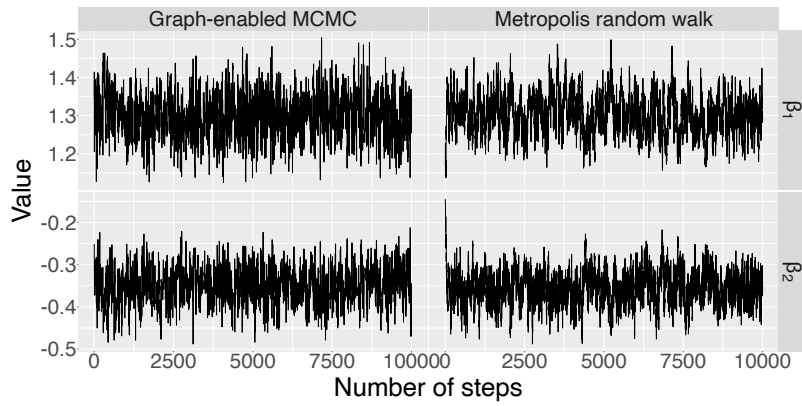


Figure 8: True and estimated posteriors in Experiment I

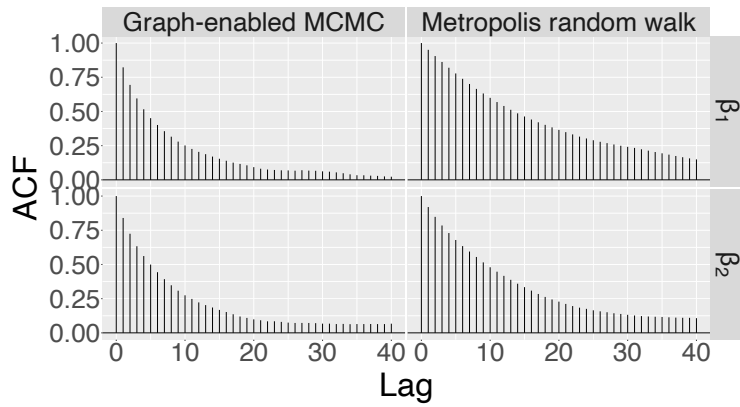
In Figures 9-11, we present MCMC convergence diagnostics (including Gelman-Rubin-Brooks plot, traceplot, and autocorrelation plot) in Experiment II.



(a) Gelman-Rubin-Brooks plots

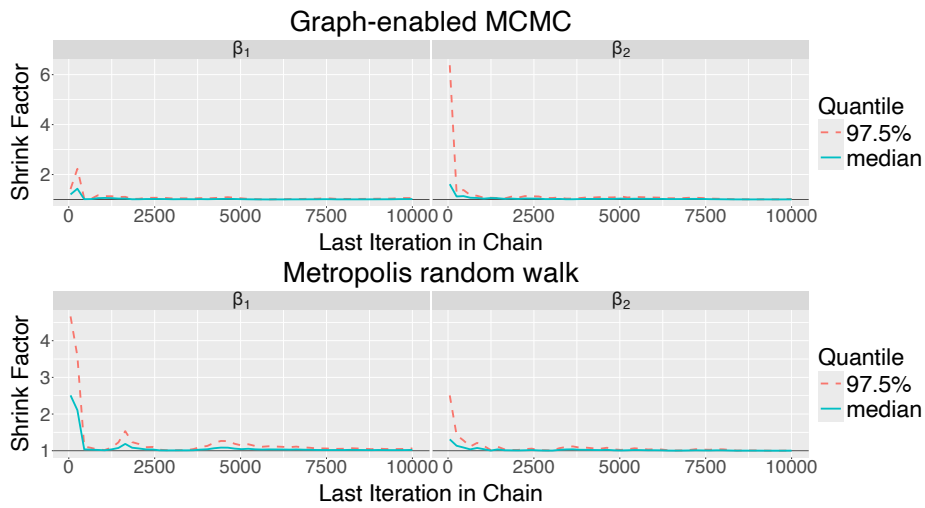


(b) Traceplots

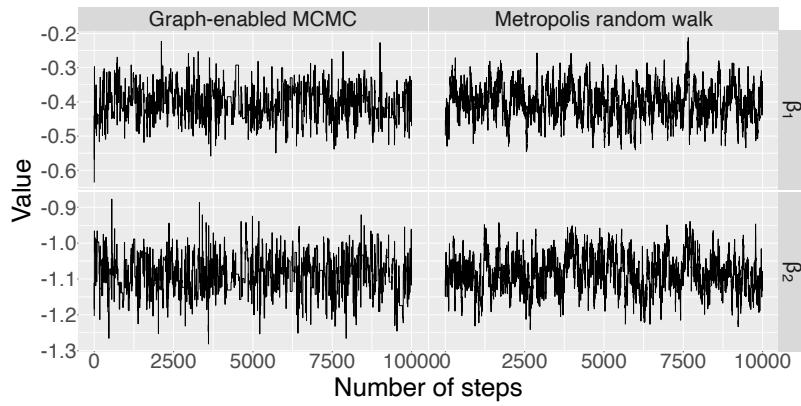


(c) Autocorrelation plots

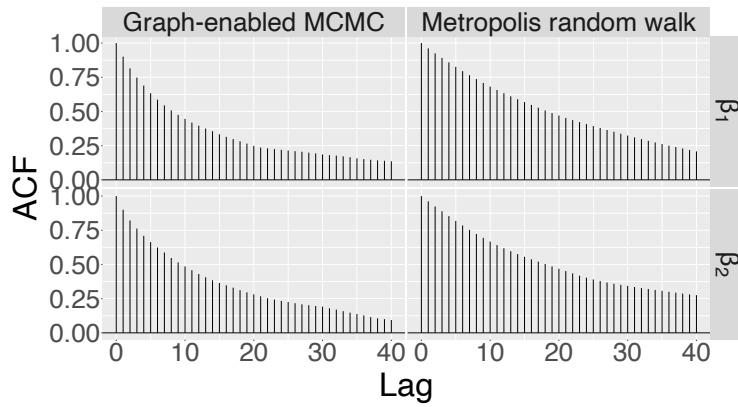
Figure 9: MCMC convergence diagnostics: Experiment II,  $d = 2$



(a) Gelman-Rubin-Brooks plots

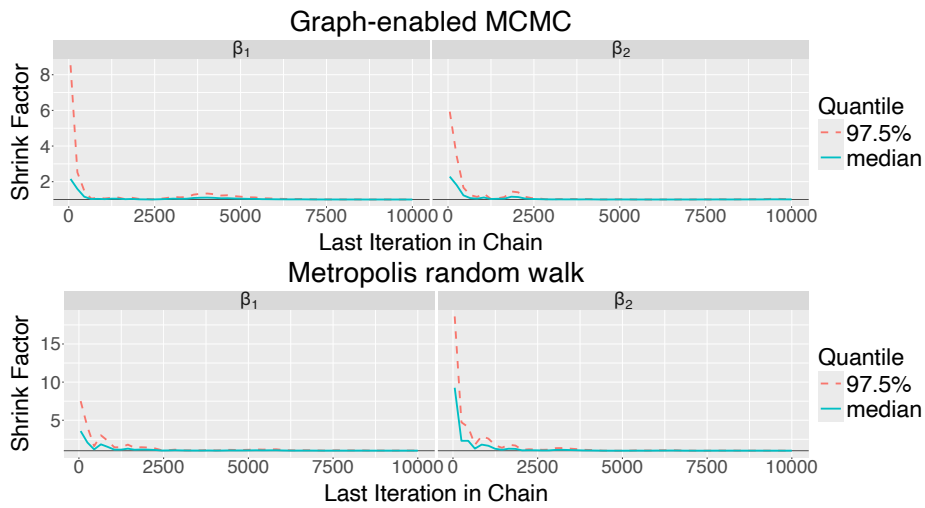


(b) Traceplots

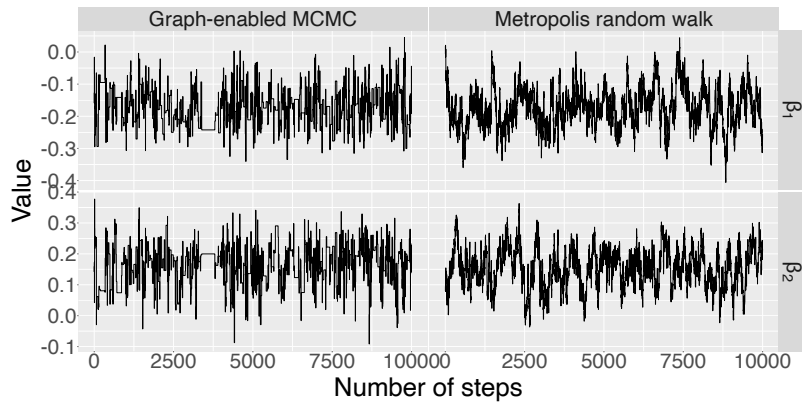


(c) Autocorrelation plots

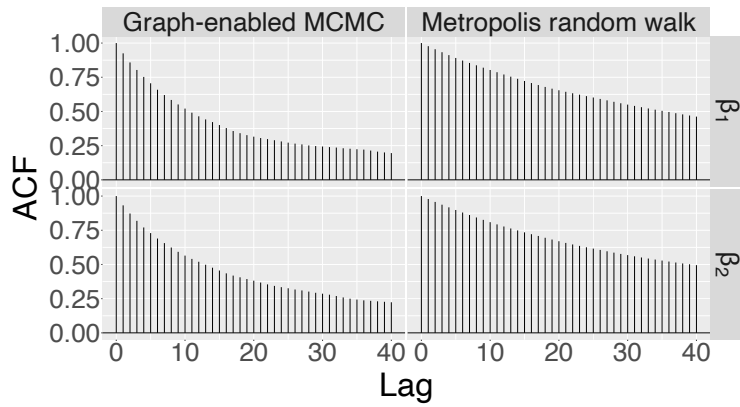
Figure 10: MCMC convergence diagnostics: Experiment II,  $d = 6$



(a) Gelman-Rubin-Brooks plots



(b) Traceplots



(c) Autocorrelation plots

Figure 11: MCMC convergence diagnostics: Experiment II,  $d = 10$

# C Details of the adaptive algorithm for prior-likelihood distributional gaps

In this section, we provide the details of the adaptive algorithm for handling prior-likelihood distributional gaps discussed in Section 6 of the paper.

We fix  $\rho' \in (0, 1)$  and  $\sigma > 0$ . The algorithm is a Markov chain on  $\tilde{\Theta}_0 \times \mathbb{R}^d$ . Initially (at step 0), we pick  $\theta_{(0)}^{(0)}$  uniformly at random from  $\Theta_0$ , and draw  $\theta_0^{(1)}$  from the distribution  $p_{\theta_{(0)}^{(0)}, h}(\cdot)$  (see equation (5) in the paper). For any  $t \in \mathbb{N}^*$ , assuming that the state at step  $t - 1$  is  $(\theta_{(t-1)}^{(0)}, \theta_{t-1}^{(1)}) \in \tilde{\Theta}_0 \times \mathbb{R}^d$ , the state at step  $t$  can be determined as follows:

- If  $\theta_{(t-1)}^{(0)} \in \Theta_0$ :
  - With probability  $\rho'$ , we do the following:
    1. With probability  $\rho$ , we draw  $\alpha_t$  uniformly from  $\Theta_0$ ; with probability  $1 - \rho$ , we draw  $\alpha_t$  uniformly from the neighbors of  $\theta_{(t-1)}^{(0)}$  in the graph  $G_k$ . Then we draw  $\tilde{\alpha}_t$  from the distribution  $p_{\alpha_t, h}(\cdot)$ .
    2. Compute the acceptance probability

$$\text{MH}_t = \min \left\{ \frac{\frac{\rho}{B} + \frac{1-\rho}{D_k(\alpha_t)} \mathbb{1}_{\{\theta_{(t-1)}^{(0)}, \alpha_t\} \in E_k}}}{\frac{\rho}{B} + \frac{1-\rho}{D_k(\theta_{(t-1)}^{(0)})} \mathbb{1}_{\{\theta_{(t-1)}^{(0)}, \alpha_t\} \in E_k}} \cdot \frac{L(\tilde{\alpha}_t | \mathbf{X})}{L(\theta_{t-1}^{(1)} | \mathbf{X})}, 1 \right\}.$$

With probability  $\text{MH}_t$ ,  $(\theta_{(t)}^{(0)}, \theta_t^{(1)}) = (\alpha_t, \tilde{\alpha}_t)$ ; otherwise  $(\theta_{(t)}^{(0)}, \theta_t^{(1)}) = (\theta_{(t-1)}^{(0)}, \theta_{t-1}^{(1)})$ .

- With probability  $1 - \rho'$ , we do the following. Compute the acceptance probability

$$\text{MH}_t = \min \left\{ \frac{(1 - \gamma)\epsilon h^d}{\gamma K \left( \frac{\theta_{t-1}^{(1)} - \theta_{(t-1)}^{(0)}}{h} \right)}, 1 \right\}.$$

With probability  $\text{MH}_t$ ,  $(\theta_{(t)}^{(0)}, \theta_t^{(1)}) = (\Delta, \theta_{t-1}^{(1)})$ ; otherwise  $(\theta_{(t)}^{(0)}, \theta_t^{(1)}) = (\theta_{(t-1)}^{(0)}, \theta_{t-1}^{(1)})$ .

- If  $\theta_{(t-1)}^{(0)} = \Delta$ :

- With probability  $\rho'$ , we do the following. Draw  $\tilde{\alpha}_t$  from  $\mathcal{N}(\theta_{t-1}^{(1)}, \sigma^2)$ , and compute the acceptance probability

$$\text{MH}_t = \min \left\{ \frac{L(\tilde{\alpha}_t | \mathbf{X})}{L(\theta_{t-1}^{(1)} | \mathbf{X})}, 1 \right\}.$$

With probability  $\text{MH}_t$ ,  $(\theta_{(t)}^{(0)}, \theta_t^{(1)}) = (\Delta, \tilde{\alpha}_t)$ ; otherwise  $(\theta_{(t)}^{(0)}, \theta_t^{(1)}) = (\theta_{(t-1)}^{(0)}, \theta_{t-1}^{(1)})$ .

- With probability  $1 - \rho'$ , we do the following. Pick  $\alpha_t$  uniformly from  $\Theta_0$ , and compute the acceptance probability

$$\text{MH}_t = \min \left\{ \frac{\gamma K \left( \frac{\theta_{t-1}^{(1)} - \alpha_t}{h} \right)}{(1 - \gamma)\epsilon h^d}, 1 \right\}.$$

With probability  $\text{MH}_t$ ,  $(\theta_{(t)}^{(0)}, \theta_t^{(1)}) = (\alpha_t, \theta_{t-1}^{(1)})$ ; otherwise  $(\theta_{(t)}^{(0)}, \theta_t^{(1)}) = (\theta_{(t-1)}^{(0)}, \theta_{t-1}^{(1)})$ .

It can be checked that the stationary distribution of  $(\theta_{(t)}^{(0)}, \theta_t^{(1)})$  is given by equation (13) in the paper. Hence the stationary distribution of  $\theta_t^{(1)}$  is given by

$$\hat{\pi}_{\gamma, \epsilon}(\theta | \mathbf{X}) \propto \left( \frac{\gamma}{B h^d} \sum_{i=1}^B K \left( \frac{\theta - \theta_i^{(0)}}{h} \right) + (1 - \gamma)\epsilon \right) L(\theta | \mathbf{X}).$$